ABSTRACT

Title of Dissertation: DYNAMICS OF SOME FERMI ACCELERATION MODELS

Jing Zhou
Doctor of Philosophy, 2020

Dissertation Directed by: Professor Dmitry Dolgopyat
Department of Mathematics

In the thesis we describe the dynamics of two variations of the Fermi acceleration models.

The first model consists of a rectangular billiard with two periodically vertically oscillating slits. A point particle bounces elastically against the billiard table and the slits. We assume that the horizontal motion of the particle is in resonance with those of the slits. In this case, we have found a mechanism of trapping regions which provides the exponential acceleration for almost all initial conditions with sufficiently high initial energy. Under an additional hyperbolicity assumption on the parameters of the system, we estimate the waiting time after which most high-energy orbits start to gain energy exponentially fast.

The second model depicts a point particle bouncing elastically against a periodically oscillating platform in a gravity field. We assume that the platform motion is piecewise smooth with one singularity. If the second derivative of the platform motion behaves well, i.e. it is either always positive or always less than the negative

of the gravitational constant, then the escaping orbits constitute a null set and the system is recurrent. However, under these assumptions, escaping orbits coexist with bounded orbits at arbitrarily high energy levels.

DYNAMICS OF SOME FERMI ACCELERATION MODELS

by

Jing Zhou

Dissertation submitted to the Faculty of the Graduate School of the
University of Maryland, College Park in partial fulfillment
of the requirements for the degree of
Doctor of Philosophy
2020

Advisory Committee:
Professor Dmitry Dolgopyat, Chair/Advisor
Professor Adam Kanigowski
Professor Giovanni Forni
Professor Michael Jakobson
Professor Vadim Kaloshin
Professor Edward Ott, Dean's Representative

Dedication

To my Mom and Dad, who have instilled in me the courage to love and explore.

Acknowledgments

First and foremost, I am eternally grateful to my academic father and friend, Dima, who taught me math, passion, discipline, respect and so much more that has helped me to reach this far. I could never imagine where I would be had he not provided a roof over my head or become the guiding star whom I needed most at the early stage of my career as a math researcher. I will always look up to him as a role model for his mathematical brilliance, enthusiasm for knowledge and generosity in helping others.

I also owe my thanks to many other professors who have enlightened and inspired me throughout my math journey. I would like to thank Vadim for leading me into the world of dynamics, Vered for proposing to me the interesting rectangular billiard model and Hong-Kun for offering her expertise on billiards for my research. I would also like to express my gratitude to Larry for giving me the opportunity to become a graduate student at our University even when I don't have a math background from undergrad.

I have greatly benefited from the company of my lovely friends in the department: Minsung, JT, Kasun, Hamid, Keagan, John and Phil. I shall never forget the days when we exchanged ideas at the student seminar and how we supported each other both intellectually and emotionally.

I am also much obliged to the staff in the department, especially Cristina and Darcy, who have made my graduate study much more enjoyable than it would have been otherwise.

The research was supported in part by Patrick and Marguerite Sung Fellowship, NSF grant DMS 1665046 and BSF grant 2016105. Part of the work was done at the Weizmann Institute, where the hospitality and excellent working conditions are gratefully appreciated.

Lastly, I would like to express my deepest gratitude for my parents and Xin, for their unswerving love and support, which have made much more blissful these many years of my pursuit for knowledge and growth.

Table of Contents

Chapter 1: Introduction

In an attempt to explain for the existence of high energy particles in cosmic rays, Fermi [17] in 1949 proposed a model in which charged particles undergo repeated reflections in moving magnetic fields. Later in 1961 Ulam [42] contended that a similar mechanism should appear in finite degree of freedom systems. He conceived a toy model where a particle travels freely and bounces elastically between two infinitely heavy walls, one fixed and the other moving periodically (c.f. Figure 1.1). Ulam [42] performed numerical experiments on a piecewise linear model and conjectured that there exist *escaping orbits*, i.e. those orbits whose energy tends to infinity with time. In addition, *bounded orbits* (i.e. those whose energy always stay bounded) and *oscillatory orbits* (i.e. those whose energy have a finite liminf but infinite limsup) might also appear in this type of models and extensive efforts have been made to examine the existence and prevalence of each of these three types of orbits in the Fermi-Ulam models and its variations (the author refers to [12, 19, 29] for surveys on this subject).

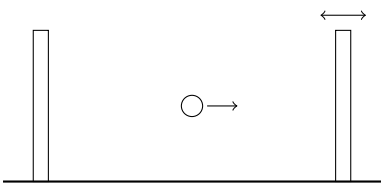

Figure 1.1: The Original Fermi-Ulam Model

Notably the KAM theory has eliminated the possibility of the existence of such escaping orbits in the Fermi-Ulam models, provided that the wall motions are sufficiently smooth [25] [38] [39], as the prevalence of invariant curves prevents energy diffusion at arbitrarily high energy levels and thus forces all orbits to be bounded.

However, unbounded solution can still be obtained in nonsmooth cases. For example, Zharnitsky [45] has found a particular type of unbounded orbits in the piecewise linear case that Ulam had considered (c.f. Figure 1.2), whose energy grows linearly in time. In the same paper, he extended this result to the "squash player's" problem [28], which is equivalent to the piecewise smooth Fermi-Ulam problem with a large velocity jump in a period. In a piecewise smooth model with one singularity (c.f. Figure 1.3), de Simoi and Dolgopyat [8] showed that there exists a parameter dichotomizing the behavior of the system: depending on whether the linear part of the limiting system at infinity is *elliptic* or *hyperbolic* (i.e. whether the absolute value of trace is less or greater than 2), bounded orbits co-exist with escaping ones in elliptic regimes while escaping orbits have zero measure but full Hausdorff dimension in hyperbolic regimes.

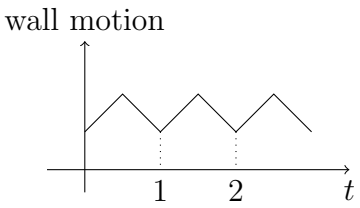

Figure 1.2: Piecewise Linear Model

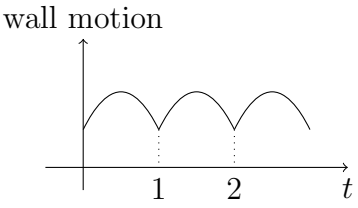

Figure 1.3: Piecewise Smooth Model with One Singularity

There are many interesting questions pertinent to the Fermi-Ulam models

with non-periodic wall motions. For instance, Zharnitsky [46] extended the KAM stability result from the periodic Fermi-Ulam models to quasi-periodic ones with Diophantine frequencies, by proving a quasi-periodic version of the Moser's twist theorem. When the Diophantine condition on the frequencies is relaxed to rational independence, Kunze and Ortega [24] showed that typically the set of initial data which lead to escaping orbits has zero Lebesgue measure.

Rich dynamical phenomena have also been observed when the motion between collisions is not free but subject to a potential. When the fixed wall is removed and a potential of the form $U = x^\alpha$ is present, Pustylnikov [37] showed that for $\alpha = 1$ (i.e. the background force is constant) there exists an open set of wall motions in the space of analytic periodic functions admitting analytic extension to a fixed strip $|\Im t| < \varepsilon$ which produce infinite measure of escaping orbits. In a model of piecewise linear oscillators (i.e. $\alpha = 2$), Ortega [33, 34] provided conditions for the existence of escaping orbits. When the wall motion is of sin-type, Dolgopyat [11] proved that for $\alpha > 1, \alpha \neq 2$ the escaping orbits do not exist, while for $\alpha < 1/3$ the escaping set has zero measure. For $\alpha < 1$ and sinuous wall motions, de Simoi [7] showed that the escaping orbits possess full Hausdorff dimension. In a Duffing equation with a time-dependent polynomial potential with one discontinuity, Levi and You [27] proved the existence of oscillatory orbits. Arnold and Zharnitsky [2] also found unbounded orbits in a pinball system with switching potentials.

Two-dimensional billiard models are natural generalizations of the one-dimensional Fermi acceleration model and can often provide chaotic orbits even in the smooth case. For example, escaping orbits were proven to exist in billiard models with

the smoothly breathing boundary [22, 23, 26]. In a Lorentz gas model [31], the average velocity of particles grows linearly in time for stochastic perturbation of scatterer boundaries and quadratically for periodic perturbation. Exponentially growing orbits for non-autonomous billiards were constructed in [21]. Shah, Turaev and Rom-Kedar [40] numerically investigated a rectangular billiard model with a moving slit. They proposed a random process approximation, i.e. the probability of jumping above or below the slit is proportional to the length of openings. They numerically verified the expected exponential growth rate for a large ensemble of initial conditions in the non-resonant case and they also numerically observed that the growth rate in the resonant case was significantly higher [40]. Later they generalized the idea to higher-dimensional time-dependent billiards and obtained a new class of numerically robust exponential accelerators [18]. Exponential acceleration is also conjectured to be generic for oscillating mushrooms [20]. However, it remains challenging to detect a positive measure set of exponentially growing orbits, and so is to study the typical behavior of the entire system.

In this thesis we describe the dynamics of two variations of the Fermi acceleration models. The first model consists of a rectangular billiard with two periodically oscillating slits. We assume that the horizontal motion of the particle is in resonance with those of the slits. This model was inspired by the previously mentioned work of Shah, Turaev and Rom-Kedar [40]. The second model depicts a ball bouncing vertically against a periodically oscillating platform in a gravity field. We assume that the platform motion is piecewise smooth with one singularity. This model is a non-smoonth modification of the one-dimensional model considered by Pustylnikov [37].

In both models, we assume that the particle is massless so that the collisions have no effect on the motions of the moving objects (i.e. the slits or the platform) and that the collisions are elastic. We record the time and the velocity immediately after each collision the ball makes against the moving objects and we study the collision map which sends the information of one collision (i.e.the time and the velocity) to the next one.

For the rectangular billiard model, we show that almost all initial conditions with sufficiently high initial velocity produce exponential energy growth in the future, provided that the relative positions of the two slits are different at the times of the two jumps such that a "trapping region" is created (c.f. Section 2.1 and Fig.3.6). Moreover, under an additional hyperbolicity assumption we estimate the waiting time after which most high-energy orbits start the exponential acceleration. We note that the rectangular billiard is pseudo-integrable as long as the ball only interacts with one slit, in the sense that the motion can be approximated by an integrable one with vanishing error as velocity tends to infinity (c.f. Section 3.2.1 for details). However the passages between left and right slit break the pseudo-integrability and create chaos, in the sense that the normal forms obtained in Section 3.2.2 can be hyperbolic. Similar mechanisms of chaos have been observed in separatrix passages and kicked oscillations [3,32,36,43,44]. We also refer to [13] for discussion of similar phenomena in the piecewise smooth setting.

For the bouncing ball in gravity model, we show that if the second derivative of the wall motion behaves, i.e. the second derivative is either always positive or always less than the negative of the gravitational constant, then the escaping orbits

have zero measure and the collision map is recurrent in the sense that almost every high energy orbit returns arbitrarily close to its initial energy level. Nevertheless, we also show that under these assumptions, escaping and bounded orbits still exist at arbitrarily high energy levels.

The thesis is organised as follows. We describe the setup and the main results for the two models in Chapter 2. The proofs of these main results are presented in Chapter 3 and Chapter 4 respectively.

The Fermi acceleration models are, by its nature, an inter-discipline subject that attracts both mathematicians and physicists. We have found a mechanism for exponential acceleration, i.e. the trapping regions, which, to the author's best knowledge, is the first result on Fermi acceleration models where robust exponential acceleration is rigorously established. From a technical viewpoint, these two models serve as excellent examples of infinite measure dynamical systems, a field that has long been proven extremely challenging and the existing literature on the subject is rare and scarce. In both models, we overcome the difficulty arising from the infinite measure phase spaces by taking a detour through the limiting dynamics, which can be either confined or projected onto compact fundamental domains (c.f. Section 3.2 and Section 4.1). The techniques from hyperbolic dynamics are explored and employed in both cases, especially the Growth Lemmas (c.f. Lemma 3.4.2 and Lemma 4.4.5) which aim at controlling the size of short unstable manifolds resulting from the nonsmooth nature of the systems.

The thesis is based on two of the author's papers: one already published [48] and the other submitted for publication [47].

Chapter 2: Main Results

2.1 A Rectangular Billiard with Moving Slits

In this section we present the first model: a rectangular billiard with two moving slits.

In our setting, the billiard table is a unit square. Two slits are moving vertically in the table with the length of left slit λ and the length of the right slit $1-\lambda$, where $\lambda \in (0,1)$ is a constant. The motion of the two slits are described by two C^2 2-periodic functions $h_L(t)$ and $h_R(t)$ respectively. A massless ball bounces elastically against the moving slits as well as the boundary of the rectangular table (c.f. Figure 2.1).

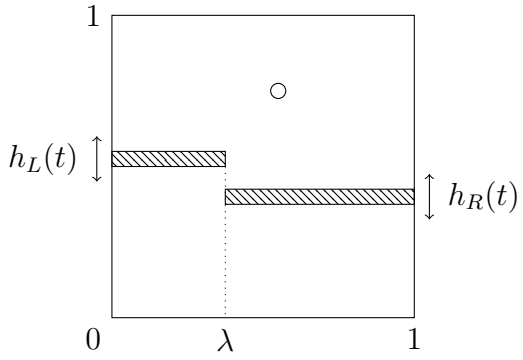

Figure 2.1: Rectangular Billiard with Moving Slits

We study the strongest resonant case. Namely, we assume that the horizontal

speed the ball is 1, so the horizontal coordinate of the ball is periodic with period 2. Hence we have 1:1 resonance between the period of moving slits and the period of the horizontal motion of the ball. The ball experiences two jumps between the left and the right parts of the table during each period. We denote by x_0 the starting horizontal position of the ball. We may assume without loss of generality that the ball starts from the left part of the table, i.e. $0 \leqslant x_0 < \lambda$. The ball jumps from the left slit to right one at time $t_1^* = \lambda - x_0$ and then from right to the left at time $t_2^* = 2 - \lambda - x_0$. We note that due to the resonance, the times t_1^*, t_2^* of jumps do not change once the parameters x_0, λ are fixed.

We record the time and the vertical velocity of the ball immediately after each collision with the slits. We exclude from our discussion the trajectories having a collision at $x = \lambda$, which constitute a null set among all the initial conditions.

For a wide range of choices in λ and x_0, the relative positions of the left and right slits are different when the ball jumps from one slit to the other at time t_1^* and t_2^* (c.f. Figure 2.2 and 3.6). A *trapping region* is created in this case and the ball starts to gain energy exponentially fast once it gets trapped.

Theorem 1. *Assume λ and x_0 are such that $h_L(t_1^*) < h_R(t_1^*)$, $h_L(t_2^*) > h_R(t_2^*)$ or $h_L(t_1^*) > h_R(t_1^*)$, $h_L(t_2^*) < h_R(t_2^*)$. Then there exists $V_* \gg 1$, which depends only on h_L and h_R, such that almost every orbit whose initial speed is greater than V_* eventually gains energy exponentially in time. In particular, the set of initial conditions (t_0, v_0) which do not enjoy exponential energy growth has finite measure.*

In the presence of a trapping region, with additional hyperbolicity assumptions

we estimate the waiting time after which most high-energy orbits start to accelerate exponentially.

We define a new function h as follows

$$h(t) = \begin{cases} h_L(t) & 0 < t < t_1^* \text{ or } t_2^* < t < 2 \\ \\ h_R(t) & t_1^* < t < t_2^*. \end{cases}$$

We introduce a new quantity Tr. If $h_L(t_1^*) < h_R(t_1^*), h_L(t_2^*) > h_R(t_2^*)$, then the lower chamber is trapping and we define in the upper chamber

$$Tr = Tr^U = \left(\frac{1-h_1^-}{1-h_1^+} - a_1\beta\right)\left(\frac{1-h_2^-}{1-h_2^+} - a_2\alpha\right) + \left(\frac{1-h_1^+}{1-h_1^-} - a_1\alpha\right)\left(\frac{1-h_2^+}{1-h_2^-} - a_2\beta\right) - a_1a_2\alpha\beta$$

where $h_i^{\pm} = h(t_i^* \pm)$, $a_i = \dot{h}_i^-(1-h_i^+) - \dot{h}_i^+(1-h_i^-)$,

$$\alpha = \left(\int_0^{t_1^*} + \int_{t_2^*}^2\right)\frac{ds}{(1-h(s))^2} \quad \text{and} \quad \beta = \int_{t_1^*}^{t_2^*}\frac{ds}{(1-h(s))^2}.$$

On the other hand, if $h_L(t_1^*) > h_R(t_1^*), h_L(t_2^*) < h_R(t_2^*)$, then the upper chamber is trapping and we define in the lower chamber

$$Tr = Tr^L = \left(\frac{h_1^-}{h_1^+} - a_1'\beta'\right)\left(\frac{h_2^-}{h_2^+} - a_2'\alpha'\right) + \left(\frac{h_1^+}{h_1^-} - a_1'\alpha'\right)\left(\frac{h_2^+}{h_2^-} - a_2'\beta'\right) - a_1'a_2'\alpha'\beta'$$

where $a_i' = \dot{h}_i^+h_i^- - \dot{h}_i^-h_i^+$, $\alpha' = \left(\int_0^{t_1^*} + \int_{t_2^*}^2\right)\frac{ds}{h(s)^2}$ and $\beta' = \int_{t_1^*}^{t_2^*}\frac{ds}{h(s)^2}$.

Theorem 2. *Assume λ and x_0 are such that the assumption in Theorem 1 holds*

and that $|Tr| > 2$. *Then there are* $K, \zeta > 0$ *such that for any* $\epsilon > 0$, *there exists* $V_0 = V_0(\epsilon)$ *and* $T = T(\epsilon)$ *such that for each* $V \geqslant V_0$ *the complement of set*

$$\left\{ (t_0, v_0) : |v_0| \in [V, V+1] : \forall t \geqslant T \quad |v(t)| \geqslant \frac{|v(T)|}{K} e^{\zeta t} \right\}$$

has measure less than ϵ, *i.e. most orbits with initial energy* $|v_0| > V_0$ *start to accelerate exponentially after time* T.

The proof of this result is constructive. In particular, T depends logarithmically on ϵ (see Equations (3.11) and (3.12)). The quantity Tr is in fact the linear part of the normal forms in Section 3.2.2 and the "hyperbolicity assumption" here means $|Trace| > 2$.

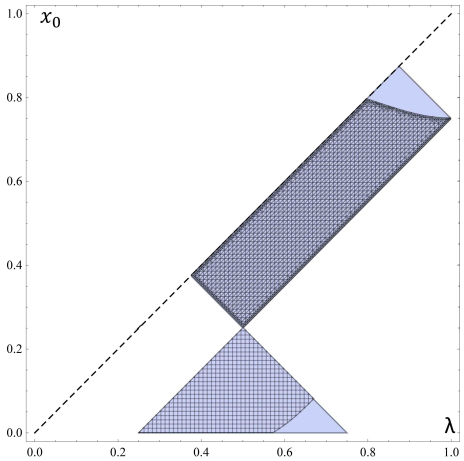

Figure 2.2: Trapping Regions

The plot of trapping regions for $h_L(t) = 0.3\cos(\pi t) + 0.5$, $h_R(t) = 0.3\sin(\pi t) + 0.5$. The blue part indicates the values of λ, x_0 for which a trapping region exists: the upper rectangle is where the upper chamber is trapping and the lower triangle is where the lower chamber is trapping. The shaded part displays where the hyperbolicity assumption $|Tr| > 2$ holds.

Example 2.1.1. To illustrate our results, we consider the case where

$$h_L(t) = 0.3\cos(\pi t) + 0.5, \quad h_R(t) = 0.3\sin(\pi t) + 0.5. \tag{2.1}$$

Then

$$\Delta(t) := h_L(t) - h_R(t) = 0.3\sqrt{2}\cos\left(\pi t + \frac{\pi}{4}\right).$$

A trapping region exists for λ, x_0 such that either

$$\Delta(\lambda - x_0) > 0, \quad \Delta(2 - \lambda - x_0) < 0 \quad \text{or} \quad \Delta(\lambda - x_0) < 0, \quad \Delta(2 - \lambda - x_0) > 0.$$

The former case is equivalent to $\lambda - x_0 < 0.25,\ 0.75 < \lambda + x_0 < 1.75$; the upper chamber is trapping and the hyperbolicity assumption holds if $|Tr^L| > 2$.

The latter case is equivalent to $\lambda - x_0 > 0.25,\ \lambda + x_0 < 0.75$; the lower chamber is trapping and the hyperbolicity assumption holds if $|Tr^U| > 2$.

Figure 2.2 demonstrates that for h_L, h_R defined above by (2.1) the assumptions of Theorems 1 and 2 hold for a sizable set of parameters.

2.2 Bouncing Ball in a Gravity Field

In this section we present the second model: bouncing ball in a gravity field. The model describes a point mass bouncing elastically against an infinitely heavy moving wall in the gravity field. The motion (height) of the wall is a piecewise smooth periodic function $f(t)$ and the gravitational constant is given by g.

We are interested in the case when the motion $f(t)$ of the wall is 1-periodic and

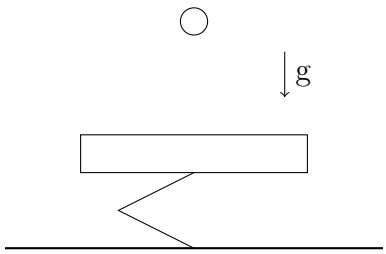

Figure 2.3: Bouncing Pingpong in Gravity Field

piecewise C^3, i.e $f(t+1) = f(t)$, $f \in C^3(0,1)$ and $\dot{f}(0+) \neq \dot{f}(1-)$. We record the time t of each collision and the velocity v immediately after each collision. Similarly to the first model, we exclude from our discussion the singular collisions at integer times, which form a null set in the (t, v)-phase cylinder. We investigate the dynamics of the system by looking at the collision map F, which sends one collision (t, v) to the next one $(\bar{t}, \bar{v})$.

We denote the second derivative of the wall motion as $k(t) = \ddot{f}(t)$. The collision map F preserves an absolutely continuous measure $\mu = wdtdv$ where $w = v - \dot{f}$ is the relative velocity after collision (c.f. Section 4.1.1).

For large velocities, the dynamics can be approximated by

$$F(t, v) = F_\infty(t, v) + \mathcal{O}\left(\frac{1}{v}\right)$$

where

$$F_\infty(t, v) = \left(t + \frac{2v}{g}, v + 2\dot{f}\left(t + \frac{2v}{g}\right)\right).$$

It is easy to verify that the limit map F_∞ is area-preserving and it covers a

map $\tilde{F}_\infty$ on the torus $\mathbb{R}/\mathbb{Z} \times \mathbb{R}/g\mathbb{Z}$

$$\tilde{F}_\infty : \begin{cases} \tilde{t}_1 = \tilde{t}_0 + \frac{2\tilde{v}_0}{g} \\ \\ \tilde{v}_1 = \tilde{v}_0 + 2\dot{f}(\tilde{t}_1) \end{cases}$$

where $\tilde{t} = t \pmod 1$, $\tilde{v} = v \pmod g$.

If the second derivative $\ddot{f}$ of the wall motion is either always positive or always less than $-g$, then the limit map $\tilde{F}_\infty$ is ergodic:

Theorem 3. *Suppose that $\ddot{f}(t) > 0$ for any $t > 0$. Then the map $\tilde{F}_\infty$ is ergodic.*

Theorem 4. *Suppose that for any $t > 0$, $\ddot{f}(t) < -g$ where g is the gravitational constant. Then the map $\tilde{F}_\infty$ is ergodic.*

We shall call a wall motion $f(t)$ *admissible* if either for all t, $\ddot{f} > 0$ or for all t, $\ddot{f} < -g$.

Remark 2.2.1. The map $\tilde{F}_\infty$ might not be ergodic if the assumptions in Theorem 3 and Theorem 4 fail. For example, when the wall motion is analytic Pustylnikov [37] found an KAM island for the limit map for an open set of analytic periodic wall motions which admit analytic extension to a strip $|\Im t| < \varepsilon$. Note that for analytic motions $\int_0^1 \ddot{f}(t)dt = 0$ so analytic motions are not admissible.

Besides the above ergodic properties, we also obtain strong statistical properties of $\tilde{F}_\infty$ under the same assumptions.

For every $x, y \in \mathbb{T}$, we define their *forward separation time* $s_+(x, y)$ to be the smallest nonnegative integer n such that x, y belongs to distinct continuity

components of $\tilde{F}_\infty^n$. We can define similarly their *backward separation time* $s_-(x,y)$ for the inverse iterates.

A function $\varphi : \mathbb{T} \to \mathbb{R}$ is said to be *dynamically Hölder continuous* if there exist $\vartheta = \vartheta(\tilde{F}_\infty) \leqslant 1$ such that

$$|\varphi|_\vartheta^+ := \sup \left\{ \frac{|\varphi(x) - \varphi(y)|}{\vartheta^{s_+(x,y)}} : x \neq y \text{ on the same unstable manifold} \right\} < \infty,$$

and that

$$|\varphi|_\vartheta^- := \sup \left\{ \frac{\varphi(x) - \varphi(y)|}{\vartheta^{s_-(x,y)}} : x \neq y \text{ on the same stable manifold} \right\} < \infty.$$

Theorem 5 (Exponential Decay of Correlations)**.** *Suppose that the wall motion is admissible. Then the map $\tilde{F}_\infty$ enjoys exponential decay of correlations for dynamically Hölder continuous observables: $\exists\ b > 0$ such that for any pair of dynamically Hölder continuous observables φ, ϕ, $\exists\ C_{\varphi,\phi}$ such that*

$$\left| \int_{\mathbb{T}} (\varphi \circ \tilde{F}_\infty^n) \phi d\tilde{\mu} - \int_{\mathbb{T}} \varphi d\tilde{\mu} \int_{\mathbb{T}} \phi d\tilde{\mu} \right| \leqslant C_{\varphi,\phi} e^{-bn}, \quad n \in \mathbb{N}.$$

We observe that for any dynamically Hölder observable φ, the following quantity is finite due to Theorem 5

$$\sigma_\varphi^2 := \sum_{n=-\infty}^{\infty} \int_{\mathbb{T}} \varphi \cdot (\varphi \circ \tilde{F}_\infty^n) d\tilde{\mu} < \infty.$$

Theorem 6 (CLT)**.** *Suppose that the wall motion is admissible. Then the map $\tilde{F}_\infty$*

satisfies central limit theorem for dynamically Hölder observables, i.e.

$$\frac{1}{\sqrt{n}} \sum_{i=0}^{n-1} \varphi \circ \tilde{F}_{\infty}^{i} \overset{dist}{\rightarrow} \mathcal{N}(0, \sigma_{\varphi}^{2})$$

where φ is dynamically Hölder with zero average $\int_{\mathbb{T}} \varphi d\tilde{\mu} = 0$.

As for the original system, under the assumptions in Theorem 3 or Theorem 4 the escaping orbit of the collision map F constitute a null set:

Theorem 7 (Null Escaping Set)**.** *Suppose that the wall motion is admissible. Then the set E of escaping orbits of F has zero measure.*

It turns out that the escaping set is exactly the dissipative part of the system and consequently under the assumptions in Theorem 3 or 4 the system is recurrent:

Corollary 8 (Recurrence)**.** *Suppose that the wall motion is admissible. Then F is recurrent, i.e. almost every orbit comes arbitrarily close to its initial point.*

However, under the assumptions in Theorem 3 or Theorem 4, escaping and bounded orbits still exist:

Theorem 9. *Suppose that $f(t)$ is admissible. Then F possesses escaping and bounded orbits with arbitrarily high energy.*

Moreover, F satisfies the following *global global mixing* property for *global functions*. We say a function Φ is *global* (or *extended*) if it is bounded, uniformly continuous and has a finite average $\bar{\Phi}$ in the following sense: for any ϵ there exists

N so large that for any rectangle $V = [0,1) \times [a,b]$ with $b - a > N$ we have

$$\left| \frac{1}{\mu(V)} \int_V \Phi d\mu - \bar{\Phi} \right| \leqslant \epsilon.$$

We denote by $\mathbb{G}_U$ the space of all such global functions.

Theorem 10 (Global Global Mixing)**.** *Suppose that the wall motion is admissible. Then F is global global mixing with respect to $\mathbb{G}_U$, i.e. for any $\Phi_1, \Phi_2 \in \mathbb{G}_U$, the following holds*

$$\lim_{n\to\infty} \limsup_{\mu(V)\to\infty} \frac{1}{\mu(V)} \int_V \Phi_1 \cdot (\Phi_2 \circ F^n) d\mu =$$
$$\lim_{n\to\infty} \liminf_{\mu(V)\to\infty} \frac{1}{\mu(V)} \int_V \Phi_1 \cdot (\Phi_2 \circ F^n) d\mu = \bar{\Phi}_1 \bar{\Phi}_2.$$

Chapter 3: A Rectangular Billiard with Moving Slits

In this Chapter, we present the proofs of the Theorems stated in Section 2.1.

3.1 Preliminaries

Since the horizontal speed of the ball stays constant, only the vertical speed contributes to the energy change of the ball. Consequently, we only need to record the time t and the vertical velocity v immediately after each collision. Let us denote by H the collision map.

For $i = 1, 2$, we denote as R_i the strip in the (t, v)-plane bounded by the singularity line $S_i = \{t = t_i^*\}$ and its image HS_i. Also let $\tilde{R}_i = H^{-1}R_i$. We subdivide the singular strips R into upper and lower chamber parts R^+ and R^-.

There are four possible scenarios when the ball makes a jump: the ball always hits the slits from above or below, the ball first hits from above then from below and vice versa.

We start with the easiest case when the ball always stays in the same chamber. Then the system is effectively equivalent to a Fermi-Ulam model with the motion (height) of the wall being the piecewise smooth 2-periodic function $h(t)$ with two jump discontinuities at t_1^* and t_2^*.

Suppose that the ball is initially in the upper chamber. We omit the subscript i as the formulas for passing through the two singularities are the same. If for $(t, v) \in \tilde{R}$ we have $h(t^*+) - h(t) < v(t^* - t) < 2 - h(t) - h(t^*)$, then the ball ends in the upper chamber after jumping and the model is equivalent to the one with a fixed ceiling and a moving floor (c.f. Figure 3.1 on the left).

Two consecutive collisions (t_n, v_n) and $(t_{n+1}, v_{n+1}) = H(t_n, v_n)$ satisfy

$$\begin{cases} v_{n+1} = v_n + 2\dot{h}(t_{n+1}) \\ 2 - h(t_n) - h(t_{n+1}) = v_n(t_{n+1} - t_n). \end{cases} \tag{3.1}$$

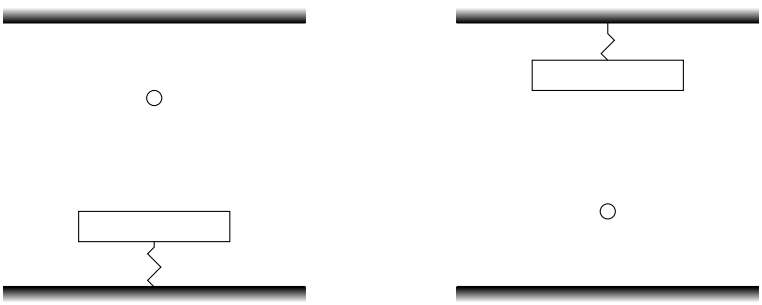

Figure 3.1: Equivalent Fermi-Ulam Models for the Upper/Lower Chambers

Similarly, suppose that the ball is initially in the lower chamber. If for $(t, v) \in \tilde{R}$ we have $h(t) - h(t^*+) < -v(t^* - t) < h(t) + h(t^*)$, then the ball ends in the lower chamber after jumping and the model is equivalent to the one with a moving ceiling and a fixed floor (c.f. Figure 3.1 on the right). Two consecutive collisions satisfy

$$\begin{cases} v_{n+1} = v_n + 2\dot{h}(t_{n+1}) \\ h(t_n) + h(t_{n+1}) = -v_n(t_{n+1} - t_n). \end{cases} \tag{3.2}$$

Now let us examine the switching cases.

Suppose that the ball is initially in the upper chamber and two consecutive collisions still follow Equation (3.1) before the ball jumps from one slit to the other. However, when the ball jumps, if the next slit is above the previous one when the ball passes through the singularities, then there is a possibility that the ball enters the lower chamber. More precisely, for $(t, v) \in \tilde{R}$, if $v(t_* - t) > 2 - h(t) - h(t_*+)$, then the ball collides with the ceiling and then enters the lower chamber (c.f. Figure 3.2 on the left); while if $v(t_* - t) < h(t_*+) - h(t)$, then the ball enters the lower chamber immediately after it leaves the previous slit (c.f. Figure 3.2 on the right).

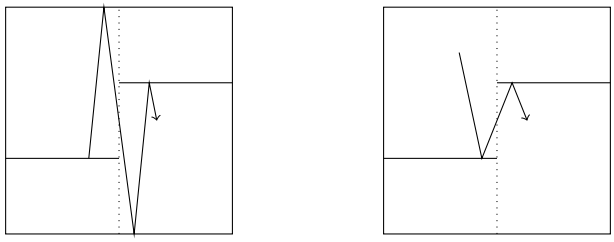

Figure 3.2: From Upper to Lower Cases

Two consecutive collisions satisfy the following Equation (3.3) in the first case

$$\begin{cases} v_n(t_{n+1} - t_n) = h(t_{n+1}) - h(t_n) + 2 \\ v_{n+1} = -v_n + 2\dot{h}(t_{n+1}) \end{cases} \tag{3.3}$$

and the following Equation (3.4) in the second case

$$\begin{cases} v_n(t_{n+1} - t) = h(t_{n+1}) - h(t_n) \\ v_{n+1} = -v_n + 2\dot{h}(t_{n+1}). \end{cases} \tag{3.4}$$

On the other hand, suppose the ball is initially in the lower chamber and two consecutive collisions still follow Equation (3.2) before the ball jumps from one slit

to the other. When the ball jumps, if the next slit is below the previous one when the ball passes through the singularities, then there is a possibility that the ball enters the upper chamber. More precisely, for $(t, v) \in \tilde{R}$, if $-v(t_* - t) > h(t) + h(t_*-)$, then the ball collides with the floor and enters the upper chamber (c.f. Figure 3.3 on the left); while if $-v(t_* - t) < h(t) - h(t_*-)$, then the ball enters the lower chamber immediately after it leaves the previous slit (c.f. Figure 3.3 on the right).

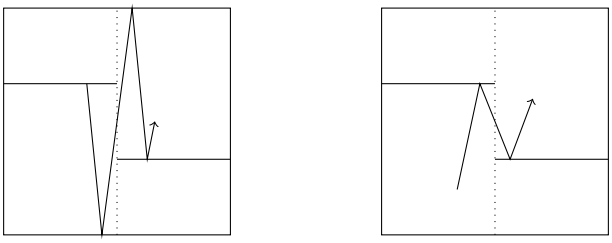

Figure 3.3: From Lower to Upper Cases

Two consecutive collisions satisfy the following Equation (3.5) in the first case

$$\begin{cases} v_n(t_{n+1} - t_n) = h(t_{n+1}) - h(t_n) - 2 \\ v_{n+1} = -v_n + 2\dot{h}(t_{n+1}) \end{cases} \tag{3.5}$$

and the following Equation (3.6) in the second case

$$\begin{cases} v_n(t_{n+1} - t) = h(t_{n+1}) - h(t_n) \\ v_{n+1} = -v_n + 2\dot{h}(t_{n+1}). \end{cases} \tag{3.6}$$

By differentiating the collision equations, we obtain that $\det H = \frac{w_n}{w_{n+1}}$ where w is the relative velocity right after collision. Consequently, the collision map H preserves the absolutely continuous measure $\mu = wdtdv$.

3.2 The Normal Form

In this section we study how the (vertical) velocity of the ball changes after one period $\Delta t = 2$ given sufficiently large initial energy. We will first approximate the collision map H with adiabatic coordinates away from singularities. Then we examine the collision dynamics when the ball passes through singularities. The change of coordinates we make is not area preserving, however, in our argument it is only important that it preserves Lebesgue measure class. Moreover, the Jacobian of our coordinate change tends to 1 as velocity tends to infinity.

3.2.1 The Adiabatic Coordinates

First we suppose that the ball collides with the slit from above and it does not make a jump at nearby collisions.

Let us denote $l(t) = 1 - h(t)$ and $\mathcal{L}_* = \int_0^2 l^{-2}(s)ds$.

Lemma 3.2.1. *For $(t, v) \notin R_i \cup \tilde{R}_i$ $(i = 1, 2)$ and $v \gg 1$, there exists an adiabatic coordinate $(\theta, I) = \Psi_U(t, v) \in \mathbb{R}/2\mathbb{Z} \times \mathbb{R}_+$ such that*

$$\theta_{n+1} = \theta_n + \frac{2}{I_n} + \mathcal{O}\left(\frac{1}{I_n^4}\right), \ I_{n+1} = I_n + \mathcal{O}\left(\frac{1}{I_n^3}\right).$$

In fact, $\theta = \theta(t) = \dfrac{2}{\mathcal{L}_*}\displaystyle\int_0^t \frac{ds}{l(s)^2} \mod 2$, $I = I(t, v) = \dfrac{\mathcal{L}_*}{2}\left(lv + l\dot{l} + \dfrac{l^2\ddot{l}}{3v}\right)$.

Proof. We can check the formula by a direct computation (c.f. Lemma 2.2 in [8]), or we can derive it in an inductive way (c.f. Section 2.2 in [10]). The basic idea is

to find higher-order adiabatic invariants. For example, observe that

$$v_{n+1} - v_n \approx -2\dot{l}(t_n), \quad t_{n+1} - t_n \approx \frac{2l(t_n)}{v_n}.$$

This leads to the Euler scheme of the following ODE

$$\frac{dv}{dt} = \frac{-v\dot{l}}{l}$$

which in turn gives us the zeroth order adiabatic invariant $I = lv$. Then we update the scheme by replacing v with I and look for the first order adiabatic invariant, etc. This scheme terminates at the second order adiabatic invariant $I = lv + l\dot{l} + \frac{l^2\ddot{l}}{3v}$.

Next, the formula for θ can be obtained reversely by solving the ODE

$$\dot{\theta}\frac{2l}{v} = \frac{2}{lv}$$

which leads to $\theta(t) = \int_0^t l^{-2}(s)ds$.

We observe that only the order v term in I is used to derive the formula for θ and it seems to produce an estimate only up to first order

$$\theta_{n+1} - \theta_n = 2/I_n + \mathcal{O}(I_n^{-2}).$$

But in fact by noting the Taylor expansion of l^{-2} and that

$$t_{n+1} - t_n = \frac{2l(t_n)}{v_n} + \frac{2l(t_n)\dot{l}(t_n)}{v_n^2} + \frac{2l(t_n)\dot{l}(t_n)^2 + 2l(t_n)^2\ddot{l}(t_n)}{v_n^3} + \mathcal{O}(v_n^{-4})$$

we obtain that

$$\begin{aligned}\int_{t_n}^{t_{n+1}} l^{-2}(s)ds &= \frac{t_{n+1}-t_n}{l_n^2} - \frac{\dot{l}_n}{l_n^3}(t_{n+1}-t_n)^2 + (\frac{\dot{l}_n^2}{l_n^4} - \frac{\ddot{l}_n}{3l_n^3})(t_{n+1}-t_n)^3 + \mathcal{O}(v_n^{-4}) \\ &= \frac{2}{l_n v_n} - \frac{2\dot{l}_n}{t_n v_n^2} + \frac{2\dot{l}_n^2 - \frac{2}{3}l_n\ddot{l}_n}{l_n v_n^3} + \mathcal{O}(v_n^{-4}) \\ &= \frac{2}{I_n} + \frac{2\dot{l}_n}{v_n I_n} + \frac{2l_n\ddot{l}_n}{3v_n^2 I_n} - \frac{2\dot{l}_n}{l_n v_n^2} + \frac{2\dot{l}_n^2 - \frac{2}{3}l_n\ddot{l}_n}{l_n v_n^3} + \mathcal{O}(v_n^{-4}) \\ &= \frac{2}{I_n} + \frac{2\dot{l}_n^2}{v_n^2 I_n} + \frac{2l_n\ddot{l}_n}{3v_n^2 I_n} + \frac{2\dot{l}_n^2 - \frac{2}{3}l_n\ddot{l}_n}{l_n v_n^3} + \mathcal{O}(v_n^{-4}) \\ &= \frac{2}{I_n} + \mathcal{O}(v_n^{-4})\end{aligned}$$

where $l_n = l(t_n)$ and $\dot{l}_n = \dot{l}(t_n)$, which produces the desired third order estimate.

Finally, we need to rescale θ (and hence I) to make θ 2 periodic. □

Next we assume that the ball collides at the slits from below and it does not make a jump at nearby collisions.

We introduce a new function $g(t) = h(t) + 1$. Then Equation (3.2) becomes the same as Equation (3.1) with g in place of h

$$\begin{cases} v_{n+1} = v_n + 2\dot{g}(t_{n+1}) \\ 2 - g(t_n) - g(t_{n+1}) = v_n(t_{n+1} - t_n) \end{cases} \tag{3.7}$$

Therefore all the computation above in Lemma 3.2.1 applies with g in the place of h.

We define $m(t) = 1 - g(t) = -h(t)$ and $\mathcal{M}_* = \int_0^2 m(s)^{-2}ds$. We have another adiabatic coordinate if the collision occurs in the lower chamber away from singularities

Lemma 3.2.2. *For $(t, v) \notin R_i \cup \tilde{R}_i$ $(i = 1, 2)$ and $v \ll -1$, there exists an adiabatic coordinate $(\zeta, J) = \Psi_L(t, v) \in \mathbb{R}/2\mathbb{Z} \times \mathbb{R}_+$ such that*

$$\zeta_{n+1} = \zeta_n + \frac{2}{J_n} + \mathcal{O}\left(\frac{1}{J_n^4}\right), \ J_{n+1} = J_n + \mathcal{O}\left(\frac{1}{J_n^3}\right).$$

In fact, $\zeta = \zeta(t) = \dfrac{2}{\mathcal{M}_*} \displaystyle\int_0^t \frac{ds}{m(s)^2} \mod 2$, $J = J(t, v) = \dfrac{\mathcal{M}_*}{2}\left(mv + m\dot{m} + \dfrac{m^2\ddot{m}}{3v}\right)$.

3.2.2 The Normal Forms

In this section we present the Poincaré map P from one singular strip to the other in four possible scenarios. We assume the initial energy of the ball is sufficiently large $|v_0| > V_*$ for some large V_* in all the cases.

3.2.2.1 The Upper-Upper Chamber Case

We begin with the upper-upper chamber case, i.e. the ball stays in the upper chamber both before and after it makes a jump. Lemma 3.2.1 already depicts the dynamics away from singularities. Now let us scrutinize what occurs near the singularities t_i^* $(i = 1, 2)$ when the ball makes a jump.

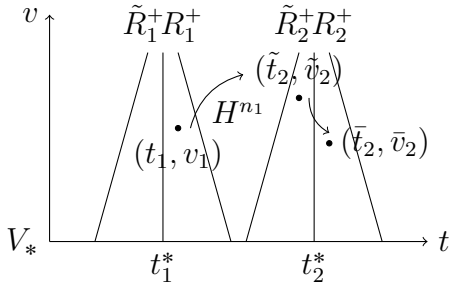

Figure 3.4: The Poincaré Map P_{UU}^{12} on the Singular Strips

For $(t_1, v_1) \in R_1^+$ with $v_1 > V_*$, we denote $(\tilde{t}_2, \tilde{v}_2) = H^{n_1}(t_1, v_1) \in \tilde{R}_2^+$, where $n_1 = [\frac{I_1}{2}(\theta_2^* - \theta_1)]$ and $\theta_2^* = \frac{2}{\mathcal{L}_*}\int_0^{t_2^*} \frac{ds}{l(s)^2}$, and $(\bar{t}_2, \bar{v}_2) = H(\tilde{t}_2, \tilde{v}_2) \in R_2^+$. Similarly, for $(t_2, v_2) \in R_2^+$ with $v_2 \gg 1$, we denote $(\tilde{t}_1, \tilde{v}_1) = H^{n_2}(t_2, v_2) \in \tilde{R}_1^+$, where $n_2 = [\frac{I_2}{2}(2 + \theta_1^* - \theta_2)]$ and $\theta_1^* = \frac{2}{\mathcal{L}_*}\int_0^{t_1^*} \frac{ds}{l(s)^2}$, and $(\bar{t}_1, \bar{v}_1) = H(\tilde{t}_1, \tilde{v}_1) \in R_1^+$.

We introduce a new pair of variables $(\tau, \mathcal{I})$ defined on the upper singular strips

$$\tau = \begin{cases} I(\theta - \theta_1^*) & \text{on } R_1^+ \\ \\ I(\theta - \theta_2^*) & \text{on } R_2^+ \end{cases}, \ \mathcal{I} = \frac{I}{\mathcal{L}_*} \text{ on } R_1^+, R_2^+$$

Now we present the Poincaré maps $P_{UU}^{12} : R_1^+ \to R_2^+$ and $P_{UU}^{21} : R_2^+ \to R_1^+$ which captures the collision dynamics when the ball travels from one singular strips to the other. We need the following constants $(i = 1, 2)$:

$$\begin{aligned}
\Delta_i &= \frac{1}{2}\frac{l(t_i^*+)}{l(t_i^*-)}\left(l(t_i^*-)\dot{l}(t_i^*+) - l(t_i^*+)\dot{l}(t_i^*-)\right), \\
\Delta_i' &= \frac{1}{8}l(t_i^*+)^2\left(l(t_i^*-)\ddot{l}(t_i^*+) - l(t_i^*+)\ddot{l}(t_i^*-)\right), \\
\Delta_i'' &= \frac{1}{24}l(t_i^*-)l(t_i^*+)\left(l(t_i^*-)\dddot{l}(t_i^*+) - l(t_i^*+)\dddot{l}(t_i^*-)\right).
\end{aligned}$$

Proposition 3.2.3 (Upper-Upper)**.** *Suppose that* $(\tau_1, \mathcal{I}_1) \in R_1^+$ *and* $\mathcal{I}_1 > V_*$*, and that*

$$h(t_2^*+) - h(t_2^*-) \lesssim l_2^-\{\mathcal{L}_*\mathcal{I}_1(\theta_2^* - \theta_1^*) - \tau_1\}_2 \lesssim 2 - h(t_2^*+) - h(t_2^*-),$$

where $\lesssim$ *means the inequality holds up to an error of order* $\mathcal{O}(\frac{1}{\mathcal{I}})$*, and* $\{\bullet\}_2 = \bullet$

mod 2. *Then the Poincaré map* $P^{12}_{UU} : R^+_1 \to R^+_2$ *is given by* $(\bar\tau_2, \bar{\mathcal{I}}_2) = G^{12}_{UU}(\tau_1, \mathcal{I}_1) + H^{12}_{UU}(\tau_1, \mathcal{I}_1) + \mathcal{O}(\mathcal{I}_1^{-2})$ *where*

$$G^{12}_{UU}(\tau_1, \mathcal{I}_1) = \left(-\frac{l^-_2}{l^+_2}\{\mathcal{L}_*\mathcal{I}_1(\theta^*_2 - \theta^*_1) - \tau_1\}_2 + 1 + \frac{l^-_2}{l^+_2}, \frac{l^+_2}{l^-_2}\mathcal{I}_1 + \Delta_2(\bar\tau_2 - 1) \right)$$

and

$$H^{12}_{UU}(\tau_1, \mathcal{I}_1) = \left(0, \Delta_2'(\bar\tau_2 - 1)^2/\mathcal{I}_1 + \Delta_2''/\mathcal{I}_1\right)$$

Similarly, suppose that $(\tau_2, \mathcal{I}_2) \in R^+_2$, $\mathcal{I}_2 > V_*$, *and that*

$$h(t^*_1+) - h(t^*_1-) \lesssim l^-_1\{\mathcal{L}_*\mathcal{I}_2(2 + \theta^*_1 - \theta^*_2) - \tau_2\}_2 \lesssim 2 - h(t^*_1+) - h(t^*_1-).$$

Then the Poincaré map $P^{21}_{UU} : R^+_2 \to R^+_1$ *is given by*

$$(\bar\tau_1, \bar{\mathcal{I}}_1) = G^{21}_{UU}(\tau_2, \mathcal{I}_2) + H^{21}_{UU}(\tau_2, \mathcal{I}_2) + \mathcal{O}(\mathcal{I}_2^{-2})$$

where

$$G^{21}_{UU}(\tau_2, \mathcal{I}_2) = \left(-\frac{l^-_1}{l^+_1}\{\mathcal{L}_*\mathcal{I}_2(2 + \theta^*_1 - \theta^*_2) - \tau_2\}_2 + 1 + \frac{l^-_1}{l^+_1}, \frac{l^+_1}{l^-_1}\mathcal{I}_2 + \Delta_1(\bar\tau_1 - 1) \right),$$

$$H^{21}_{UU}(\tau_2, \mathcal{I}_2) = \left(0, \Delta_1'(\bar\tau_1 - 1)^2/\mathcal{I}_2 + \Delta_1''/\mathcal{I}_2\right)$$

and $l^\pm_i = l(t^*_i \pm)$.

Proof. We only derive the formula for P^{12}_{UU}. The formula for P^{21}_{UU} can be obtained in a similar fashion.

For the ease of notation we drop the sub/superscripts whenever they are clear from the context. Note that near the jump discontinuity at t^*

$$
\begin{aligned}
l(\tilde{t}^*) &= l_-(t^*) + \dot{l}_-(\tilde{t} - t^*) + \frac{1}{2}\ddot{l}_-(t^*)(\tilde{t} - t^*)^2 + \mathcal{O}(\tilde{v}^{-3}),\\
l(\tilde{t}^*) &= l_+(t^*) + \dot{l}_+(\bar{t} - t^*) + \frac{1}{2}\ddot{l}_+(t^*)(\bar{t} - t^*)^2 + \mathcal{O}(\tilde{v}^{-3}),\\
\dot{l}(\tilde{t}^*) &= \dot{l}_-(t^*) + \ddot{l}_-(\tilde{t} - t^*) + \mathcal{O}(\tilde{v}^{-2}),\\
\dot{l}(\tilde{t}^*) &= \dot{l}_+(t^*) + \ddot{l}_+(\bar{t} - t^*) + \mathcal{O}(\tilde{v}^{-2}),\\
\ddot{l}(\tilde{t}^*) &= \ddot{l}_-(t^*) + \mathcal{O}(\tilde{v}^{-1}),\\
\ddot{l}(\tilde{t}^*) &= \ddot{l}_+(t^*) + \mathcal{O}(\tilde{v}^{-1}),
\end{aligned}
$$

and that

$$\bar{v} = \tilde{v} - 2\dot{l}(\bar{t}), \quad \bar{t} - \tilde{t} = \frac{l(\bar{t}) + l(\tilde{t})}{\bar{v}}.$$

Hence by solving iteratively the implicit equation we attain

$$\bar{t} - \tilde{t} = \frac{l_+ + l_-}{\tilde{v}} + (\dot{l}_+ + \dot{l}_-)\frac{\bar{t} - t^*}{\tilde{v}} - \frac{\dot{l}_-(l_+ + l_-)}{\tilde{v}^2} + \mathcal{O}(\tilde{v}^{-3}).$$

By a straightforward but tedious computation we arrive at

$$
\begin{aligned}
2\mathcal{L}_*^{-1}\left(\frac{l_-}{l_+}\bar{I}-\tilde{I}\right) &= (l_+\dot{l}_- - l_-\dot{l}_+) - \frac{l_+\dot{l}_- - l_-\dot{l}_+}{l_+}(\bar{t}-t^*)\bar{v} \\
&\quad + (l_+\ddot{l}_- - l_-\ddot{l}_+ + \frac{l_-}{l_+}\dot{l}_+^2 - \dot{l}_-\dot{l}_+)(\bar{t}-t^*) \\
&\quad + \left(\frac{l_-}{3}(l_+\ddot{l}_+ - l_-\ddot{l}_-) + \frac{\ddot{l}_-}{2}(l_-^2 - l_+^2)\right)\frac{1}{\bar{v}} \\
&\quad - \frac{l_+\ddot{l}_- - l_-\ddot{l}_+}{2l_+}(\bar{t}-t^*)^2\bar{v} + \mathcal{O}(\tilde{v}^{-2}) \\
&= \frac{l_-\dot{l}_+ - l_+\dot{l}_-}{l_+}\left((\bar{t}-t^*)\bar{v}\big(1+\frac{\dot{l}_+}{\bar{v}}\big) - l_+\right) \\
&\quad + \frac{l_-\ddot{l}_+ - l_+\ddot{l}_-}{2l_+\bar{v}}\left(\big((\bar{t}-t^*)\bar{v} - l_+\big)^2 + \frac{l_-l_+(l^-\ddot{l}_- - l_+\ddot{l}_+)}{3(l_-\ddot{l}_+ - l_+\ddot{l}_-)}\right) + \mathcal{O}(\tilde{v}^{-2}).
\end{aligned}
$$

It can be checked directly by Taylor expanding $\bar{I}$ and $\bar{\theta}$ that

$$
\bar{\tau} = \bar{I}(\bar{\theta}-\theta_2^*) = \frac{1}{l_+}\left((\bar{t}-t^*)\bar{v} + \dot{l}_+(\bar{t}-t^*)\right) + \mathcal{O}(\tilde{v}^{-2}).
$$

Thus eventually we have

$$
\bar{\mathcal{I}} = (l_+/l_-)\tilde{\mathcal{I}} + \Delta(\bar{\tau}-1) + \Delta'(\bar{\tau}-1)^2/\tilde{\mathcal{I}} + \Delta''/\tilde{\mathcal{I}} + \mathcal{O}(\tilde{\mathcal{I}}^{-2}).
$$

Now we compute $\bar{\tau}$. Observe that

$$
\bar{\tau} = \frac{\bar{v}+\dot{l}_+}{l_+}(\bar{t}-t^*) + \mathcal{O}(\bar{v}^{-2}),\ \tilde{I}(\tilde{\theta}-\tilde{\theta_2^*}) = \frac{\tilde{v}+\dot{l}_-}{l_-}(\tilde{t}-t^*) + \mathcal{O}(\bar{v}^{-2}).
$$

Therefore

$$\begin{aligned}
l_+\bar{\tau} &= ((\bar{t}-\tilde{t})+(\tilde{t}-t^*))(\tilde{v}+\dot{l}_- - (\dot{l}_- + \dot{l}_+)) + \mathcal{O}(\tilde{v}^{-2}) \\
&= (\tilde{t}-t^*)(\tilde{v}+\dot{l}_-) + (\bar{t}-\tilde{t})(\tilde{v}+\dot{l}_-) - (\bar{t}-t^*)(\dot{l}_- + \dot{l}_+) + \mathcal{O}(\tilde{v}^{-2}) \\
&= l_-\tilde{I}(\tilde{\theta}-\tilde{\theta}_2^*) + \frac{l_- + l_+}{\tilde{v}}(\tilde{v}+\dot{l}_-) + (\dot{l}_- + \dot{l}_+)(\bar{t}-t^*) \\
&- \frac{\dot{l}_-(l_- + l_+)}{\tilde{v}} - (\bar{t}-t^*)(\dot{l}_- + \dot{l}_+) + \mathcal{O}(\tilde{v}^{-2}) \\
&= l_-\tilde{I}(\tilde{\theta}-\tilde{\theta}_2^*) + l_- + l_+ + \mathcal{O}(\tilde{v}^{-2}),
\end{aligned}$$

which gives

$$\bar{\tau} = (l_-/l_+)\tilde{I}(\tilde{\theta}-\theta_2^*) + 1 + l_-/l_+ + \mathcal{O}(\tilde{I}^{-2}).$$

But Lemma 3.2.1 implies that

$$\tilde{I} = I + \mathcal{O}(I^{-2}), \quad \tilde{\theta} = \theta + \frac{2n_1}{I} + \mathcal{O}(I^{-3})$$

hence we have

$$\tilde{I}(\tilde{\theta}-\theta_2^*) = \tau + 2n_1 + I(\theta_1^* - \theta_2^*) + \mathcal{O}(I^{-2})$$

where $n_1 = [\frac{I_1}{2}(\theta_2^* - \theta_1)]$.

We hitherto complete the proof of the formula for P_{UU}^{12}. □

3.2.2.2 The Lower-Lower Chamber Case

We present here the mirror case to Section 3.2.2.1, i.e. when the ball stays in the lower chamber both before and after it makes a jump.

We need the following constants ($i = 1, 2$)

$$\zeta_i^* = \frac{2}{M_*}\int_0^{t_i^*} m(s)^{-2} ds$$
$$\Upsilon_i = \frac{1}{2}\frac{m_i^+}{m_i^-}(m_i^- \dot{m}_i^+ - m_i^+ \dot{m}_i^-)$$
$$\Upsilon_i' = \frac{1}{8} m_i^{+2}(m_i^- \ddot{m}_i^+ - m_i^+ \ddot{m}_i^-)$$
$$\Upsilon_i'' = \frac{1}{24} m_i^- m_i^+ (m_i^- \dddot{m}_i^- - m_i^+ \dddot{m}_i^+)$$

We introduce a new pair of variables $(\rho, \mathcal{J})$ on the lower singular strips, which is the counterpart of $(\tau, \mathcal{I})$ as follows

$$\rho = \begin{cases} J(\zeta - \zeta_1^*) & \text{on } R_1^- \\ \\ J(\zeta - \zeta_2^*) & \text{on } R_2^- \end{cases}, \ \mathcal{J} = \frac{J}{\mathcal{M}_*} \text{ on } R_1^-, R_2^-$$

Proposition 3.2.4 (Lower-Lower)**.** *Suppose that* $(\rho_1, \mathcal{J}_1) \in R_1^-$*, and* $\mathcal{J}_1 > V_*$*, and that*

$$h(t_2^*-) - h(t_2^*+) \lesssim -m_2^-\{\mathcal{M}_* \mathcal{J}_1(\zeta_2^* - \zeta_1^*) - \rho_1\}_2 \lesssim h(t_2^*-) + h(t_2^*+).$$

Then the Poincaré map $P_{LL}^{12} : R_1^- \to R_2^-$ *is given by*

$$(\bar{\rho}_2, \bar{\mathcal{J}}_2) = G_{LL}^{12}(\rho_1, \mathcal{J}_1) + H_{LL}^{12}(\rho_1, \mathcal{J}_1) + + \mathcal{O}(\mathcal{J}_1^{-2})$$

where

$$G^{12}_{LL}(\rho_1, \mathcal{J}_1) = \left(-\frac{m_2^-}{m_2^+}\{\mathcal{M}_* \mathcal{J}_1(\zeta_2^* - \zeta_1^*) - \rho_1\}_2 + 1 + \frac{m_2^-}{m_2^+}, \frac{m_2^+}{m_2^-}\mathcal{J}_1 + \Upsilon_2(\bar{\rho}_2 - 1) \right)$$

and

$$H^{12}_{LL}(\rho_1, \mathcal{J}_1) = \left(0, \Upsilon_2'(\bar{\rho}_2 - 1)^2/\mathcal{J}_1 + \Upsilon_2''/\mathcal{J}_1\right).$$

Similarly, suppose that $(\rho_2, \mathcal{J}_2) \in R_2^-$ *and* $\mathcal{J}_2 > V_*$*, and that*

$$h(t_1^*-) - h(t_1^*+) \lesssim -m_1^-\{\mathcal{M}_* \mathcal{J}_2(2 + \zeta_1^* - \zeta_2^*) - \rho_2\}_2 \lesssim h(t_1^*-) + h(t_1^*+).$$

Then the Poincaré map $P^{21}_{LL} : R_2^- \to R_1^-$ *is given by*

$$(\bar{\rho}_1, \bar{\mathcal{J}}_1) = G^{21}_{LL}(\rho_2, \mathcal{J}_2) + H^{21}_{LL}(\rho_2, \mathcal{J}_2) + +\mathcal{O}(\mathcal{J}_2^{-2})$$

where

$$G^{21}_{LL}(\rho_2, \mathcal{J}_2) = \left(-\frac{m_1^-}{m_1^+}\{\mathcal{M}_* \mathcal{J}_2(2 + \zeta_1^* - \zeta_2^*) - \rho_2\}_2 + 1 + \frac{m_1^-}{m_1^+}, \frac{m_1^+}{m_1^-}\mathcal{J}_2 + \Upsilon_1(\bar{\rho}_1 - 1) \right),$$

$$H^{21}_{LL}(\rho_2, \mathcal{J}_2) = \left(0, \Upsilon_1'(\bar{\rho}_1 - 1)^2/\mathcal{J}_2 + \Upsilon_1''/\mathcal{J}_2\right),$$

and $m_i^{\pm} = m(t_i^*\pm)$.

3.2.2.3 The Upper-Lower Chamber Case

Now we suppose that $(\tilde{t}, \tilde{v}) \in \tilde{R}$ and that the ball is in the upper chamber. Also we assume that the next wall is above the previous one when the ball passes through the singularity at $t = t_*$: $h(t_*-) < h(t_*+)$. Also we denote $(\bar{t}, \bar{v}) = H(\tilde{t}, \tilde{v})$.

If $\tilde{v}(t_* - \tilde{t}) > 2 - h(\tilde{t}) - h(t_*+)$, then the ball collides with the ceiling and then enters the lower chamber (c.f. Figure 3.2 on the left).

Rather than resorting to the detailed computation as we have done in the constant chamber cases, we insert an imaginary stationary slit, whose length is negligible, at the height $h_* = 1 - \tilde{v}(t_* - \tilde{t}) + l(\tilde{t})$, so that the two consecutive collisions at the moving slits are concatenated by two fictional collisions at the imaginary wall, to which the Upper-Upper and Lower-Lower formulas readily apply.

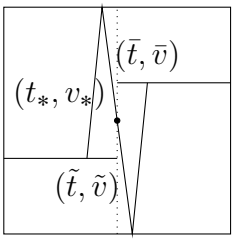

Figure 3.5: The Imaginary Stationary Wall

More precisely, as the ball leaves the previous slit at time $\tilde{t}$ with velocity $\tilde{v}$, it collides against the imaginary tiny slit at time t_* and the outgoing velocity is still $v_* = \tilde{v}$ as the slit is stationary. Meanwhile we also imagine that the ball leaves from below the fictional slit at time t_* with velocity $v_* = -\tilde{v}$ (with an abuse of notation), then it collides at the next moving slit at time $\bar{t}$ with outgoing velocity $\bar{v}$.

Let us denote $I_* = I(t_*, v_*)$, etc. We will need the following constants

$$\begin{aligned}
\kappa_{Ii} &= \frac{1}{2} m_+ (\dot{m}_+ - m_+ \dot{l}_-/l_-) \\
\kappa'_{Ii} &= \frac{1}{2} m_+ \dot{l}_-/l_- \\
\kappa''_{Ii} &= \frac{1}{8} m_+ \ddot{l}_- (1 - \frac{1}{3} l_-^2) \\
\kappa'''_{Ii} &= \frac{1}{4} m_+^2 (\ddot{l}_- + \frac{1}{6} l_- \ddot{m}_+) \\
\kappa''''_{Ii} &= \frac{1}{8} m_+^3 \ddot{l}_- \\
\kappa'''''_{Ii} &= \frac{1}{8} m_+^2 \ddot{m}_+ l_-
\end{aligned}$$

where i indicates that $l(t)$ and $m(t)$ are evaluated at $t = t_i^*$ $(i = 1, 2)$.

Then the dynamics between the singular strips is captured by the following formula:

Proposition 3.2.5 (Upper-Lower I)**.** *Assume that* $(\tau_1, \mathcal{I}_1) \in R_1^+$ *with* $\mathcal{I}_1 > V_*$ *and that*

$$l_2^- \{\mathcal{L}_* \mathcal{I}_1 (\theta_2^* - \theta_1^*) - \tau_1\}_2 \gtrsim 2 - h(t_2^*+) - h(t_2^*-).$$

Then the Poincaré map $P_{ULI}^{12} : R_1^+ \to R_2^-$ *is given by*

$$(\bar{\rho}_2, \bar{\mathcal{J}}_2) = G_{ULI}^{12}(\tau_1, \mathcal{I}_1) + H_{ULI}^{12}(\tau_1, \mathcal{I}_1) + \mathcal{O}(\mathcal{I}_1^{-2})$$

where

$$G^{12}_{ULI}(\tau_1, \mathcal{I}_1) = \left(\frac{l_2^-}{m_2^+} \{\mathcal{L}_* \mathcal{I}_1 (\theta_2^* - \theta_1^*) - \tau_1\}_2 + \frac{m_2^+ - l_2^- - 1}{m_2^+}, \right.$$
$$\left. - \frac{m_2^+}{l_2^-} \mathcal{I}_1 + \kappa_{I2}(\bar{\rho}_2 - 1) - \kappa'_{I2} \right)$$

and

$$H^{12}_{ULI}(\tau_1, \mathcal{I}_1) = \left(0, \frac{\kappa''_{I2}}{\mathcal{I}_1} + \kappa'''_{I2} \frac{\bar{\rho}_2 - 1}{I_1} + \kappa''''_{I2} \frac{(\bar{\rho}_2 - 1)^2}{\mathcal{I}_1} - \kappa'''''_{I2} \frac{(\bar{\rho}_2 - 1)^3}{\mathcal{I}_1} \right).$$

Similarly, assume that $(\tau_2, \mathcal{I}_2) \in R_2^+$ *with* $\mathcal{I}_2 > V_*$ *and that*

$$l_1^- \{\mathcal{L}_* \mathcal{I}_2 (2 + \theta_1^* - \theta_2^*) - \tau_2\}_2 \gtrsim 2 - h(t_1^* +) - h(t_1^* -).$$

Then the Poincaré map $P^{21}_{ULI} : R_2^+ \to R_1^-$ *is given by*

$$(\bar{\rho}_1, \bar{\mathcal{J}}_1) = G^{21}_{ULI}(\tau_2, \mathcal{I}_2) + H^{21}_{ULI}(\tau_2, \mathcal{I}_2) + \mathcal{O}(\mathcal{I}_2^{-2})$$

where

$$G^{21}_{ULI}(\tau_2, \mathcal{I}_2) = \left(\frac{l_1^-}{m_1^+} \{\mathcal{L}_* \mathcal{I}_2 (2 + \theta_1^* - \theta_2^*) - \tau_2\}_2 + \frac{m_1^+ - l_1^- - 1}{m_1^+}, \right.$$
$$\left. - \frac{m_1^+}{l_1^-} \mathcal{I}_2 + \kappa_{I1}(\bar{\rho}_1 - 1) - \kappa'_{I1} \right)$$

and

$$H^{21}_{ULI}(\tau_2, \mathcal{I}_2) = \left(0, \frac{\kappa''_{I1}}{\mathcal{I}_2} + \kappa'''_{I1}\frac{\bar{\rho}_1 - 1}{\mathcal{I}_2} + \kappa''''_{I1}\frac{(\bar{\rho}_1 - 1)^2}{\mathcal{I}_2} - \kappa'''''_{I1}\frac{(\bar{\rho}_1 - 1)^3}{\mathcal{I}_2}\right).$$

Proof. We present the proof of P^{12}_{ULI}. The formula for P^{21}_{ULI} can be obtained similarly. We suppress the sub/superscripts whenever they are clear from the context.

We imagine that the ball collides at the fictional stationary wall at time t_* with outgoing velocity $v_* = \tilde{v}$. Then $l_* = 1 - h_* = \tilde{v}(t_* - \tilde{t}) - l(\tilde{t})$ and we have

$$I_* = \frac{L_*}{2} l_* \tilde{v},\ \tau_* = 0.$$

From the Upper-Upper formula,

$$\tau_* = \frac{l_-}{l_*}\tilde{I}(\tilde{\theta} - \theta^*_2) + 1 + \frac{l_-}{l_*} + \mathcal{O}(v^{-2})$$

$$I_* = \frac{l_*}{l_-}\tilde{I} + \frac{L_* l_*^2}{2l_-}\dot{l}_- - \frac{L_*^2 l_*^3 \ddot{l}_-}{8\tilde{I}} + \frac{L_*^2 l_*^2 l_* \ddot{l}_-}{24\tilde{I}} + \mathcal{O}(v^{-2}).$$

Now we imagine that the ball leaves from below the fictional stationary wall at time t_* with outgoing velocity $v_* = -\tilde{v}$ (with an abuse of notation). Then $m_* = -m(\bar{t}) - v(\bar{t} - t_*)$ and we have

$$J_* = -\frac{M_*}{2} m_* \tilde{v},\ \rho_* = 0.$$

From the Lower-Lower formula,

$$\bar{\rho} = 1 + \frac{m_*}{m_+} + \mathcal{O}(v^{-2})$$

$$\bar{J} = \frac{m_+}{m_*} J_* + \frac{M_*}{2} m_+ \dot{m}_+ (\bar{\rho} - 1) + \frac{M_*^2}{8J_*} m_+^2 m_* \ddot{m}_+ (\bar{\rho} - 1)^2 - \frac{M_*^2}{24J_*} m_+^2 m_* \ddot{m}_+ + \mathcal{O}(v^{-2}).$$

We observe that

$$\begin{aligned} l_* &= v(t_* - \tilde{t}) - l(\tilde{t}) \\ &= v(t_* - \tilde{t}) - l_- - \dot{l}_-(\tilde{t} - t_*) + \mathcal{O}(v^{-2}) \\ &= -(\tilde{v} + \dot{l}_-)(t_* - \tilde{t}) - l_- + \mathcal{O}(v^{-2}) \\ &= -l_- \tilde{I}(\tilde{\theta} - \theta_2^*) - l_- + \mathcal{O}(v^{-2}) \end{aligned}$$

and that

$$\begin{aligned} m_* &= -m(\bar{t}) - v(\bar{t} - t_*) \\ &= -m_+ - \dot{m}_+(\bar{t} - t_*) + (\bar{v} + 2\dot{m}_+)(\bar{t} - t_*) + \mathcal{O}(v^{-2}) \\ &= -m_+ + (\bar{v} + \dot{m}_+)(\bar{t} - t_*) + \mathcal{O}(v^{-2}) \\ &= -m_+ + m_+ \bar{\rho} + \mathcal{O}(v^{-2}) \end{aligned}$$

Since $m_* = l_* - 1$,

$$\bar{\rho} = -\frac{l_-}{m_+} \tilde{I}(\tilde{\theta} - \theta_2^*) + \frac{m_+ - l_- - 1}{m_+} + \mathcal{O}(v^{-2}).$$

Finally the relation between I_* and J_*, together with Lemma 3.2.1, produces the formula for $\bar{J}$. □

If $v(t_*-\tilde{t}) < h(t_*+)-f(\tilde{t})$, then the ball enters the lower chamber immediately after it leaves the previous slit (c.f. Figure 3.2 on the right).

The imaginary wall trick no longer applies, so we have to return to the direct computation.

We need the following constants

$$\begin{aligned}
\kappa''_{\mathrm{IIi}} &= \frac{1}{4}m_+^2\ddot{l}_- \\
\kappa'''_{\mathrm{IIi}} &= \frac{1}{8}m_+^2(l_-\dddot{m}_+ - m_+\ddot{l}_-) \\
\kappa''''_{\mathrm{IIi}} &= \frac{1}{24}m_+l_-(l_-^2\ddot{l}_- - l_-m_+\dddot{m}_+ - 3\ddot{l}_-)
\end{aligned}$$

where i indicates that $l(t)$ and $m(t)$ are evaluated at $t = t_i^*$ $(i = 1, 2)$.

Proposition 3.2.6 (Upper-Lower II)**.** *Assume that* $(\tau_1, \mathcal{I}_1) \in R_1^+$ *with* $\mathcal{I}_1 > V_*$ *and that*

$$h(t_2^*+) - h(t_2^*-) \gtrsim l_2^-\{\mathcal{L}_*\mathcal{I}_1(\theta_2^* - \theta_1^*) - \tau_1\}_2.$$

Then the Poincaré map $P_{UL\mathrm{II}}^{12} : R_1^+ \to R_2^-$ *is given by*

$$(\bar{\rho}_2, \bar{\mathcal{J}}_2) = G_{UL\mathrm{II}}^{12}(\tau_1, \mathcal{I}_1) + H_{UL\mathrm{II}}^{12}(\tau_1, \mathcal{I}_1) + \mathcal{O}(\mathcal{I}_1^{-2})$$

where

$$G^{12}_{ULII}(\tau_1,\mathcal{I}_1)=\left(\frac{l_2^-}{m_2^+}\{\mathcal{L}_*\mathcal{I}_1(\theta_2^*-\theta_1^*)-\tau_1\}_2+\frac{m_2^+-l_2^-+1}{m_2^+},\right.$$
$$\left.-\frac{m_2^+}{l_2^-}\mathcal{I}_1+\kappa_{\mathrm{I}2}(\bar\rho_2-1)+\kappa'_{\mathrm{I}2}\right)$$

and

$$H^{12}_{ULII}(\tau_1,\mathcal{I}_1)=\left(0,-\kappa''_{\mathrm{II}2}\frac{\bar\rho_2-1}{\mathcal{I}_1}-\kappa'''_{\mathrm{II}2}\frac{(\bar\rho_2-1)^2}{\mathcal{I}_1}-\frac{\kappa''''_{\mathrm{II}2}}{\mathcal{I}_1}\right).$$

Similarly, assume that $(\tau_2,\mathcal{I}_2)\in R_2^+$ *with* $\mathcal{I}_2>V_*$ *and that*

$$h(t_1^*+)-h(t_1^*-)\gtrsim l_1^-\{\mathcal{L}_*\mathcal{I}_2(2+\theta_1^*-\theta_2^*)-\tau_2\}_2.$$

Then the Poincaré map $P^{21}_{ULII}:R_2^+\to R_1^-$ *is given by*

$$(\bar\rho_1,\bar{\mathcal{J}}_1)=G^{21}_{ULII}(\tau_2,\mathcal{I}_2)+H^{21}_{ULII}(\tau_2,\mathcal{I}_2)+\mathcal{O}(\mathcal{I}_2^{-2})$$

where

$$G^{21}_{ULII}(\tau_2,\mathcal{I}_2)=\left(\frac{l_1^-}{m_1^+}\{\mathcal{L}_*\mathcal{I}_2(2+\theta_1^*-\theta_2^*)-\tau_2\}_2+\frac{m_1^+-l_1^-+1}{m_1^+},\right.$$
$$\left.-\frac{m_1^+}{l_1^-}\mathcal{I}_2+\kappa_{\mathrm{I}1}(\bar\rho_1-1)+\kappa'_{\mathrm{I}1}\right)$$

and

$$H^{21}_{ULII}(\tau_2,\mathcal{I}_2)=\left(0,-\kappa''_{\mathrm{II}1}\frac{\bar\rho_1-1}{\mathcal{I}_2}-\kappa'''_{\mathrm{II}1}\frac{(\bar\rho_1-1)^2}{\mathcal{I}_2}-\frac{\kappa''''_{\mathrm{II}1}}{\mathcal{I}_2}\right).$$

Proof. Again we only prove the formula for P^{12}_{ULII}.

We have from Equation (3.4) that

$$
\begin{aligned}
& v(\bar{t}-\tilde{t}) = h(\bar{t}) - h(\tilde{t}) \\
\implies & \tilde{v}((\bar{t}-t_*) - (\tilde{t}-t_*)) = -m(\bar{t}) + l(\tilde{t}) - 1 \\
\implies & m_+ - (\bar{v} + \dot{m}_+)(\bar{t}-t_*) = (\tilde{v} + \dot{l}_-)(\tilde{t}-t_*) + l_- - 1 + \mathcal{O}(v^{-2}) \\
\implies & m_+ - m_+\bar{\rho} = l_-\tilde{I}(\tilde{\theta} - \theta_2^*) + l_- - 1 + \mathcal{O}(v^{-2}) \\
\implies & \bar{\rho} = -\frac{l_-}{m_+}\tilde{I}(\tilde{\theta} - \theta_2^*) + \frac{m_+ - l_- + 1}{m_+} + \mathcal{O}(v^{-2})
\end{aligned}
$$

The computation is similar to that in the proof of Proposition 3.2.3. So we just list the key steps.

We observe that

$$
\begin{aligned}
2\mathcal{M}_*^{-1}\bar{J} &= \bar{m}\bar{v} + \bar{m}\dot{\bar{m}} + \frac{\bar{m}^2\ddot{\bar{m}}}{3\bar{v}} \\
&= m_+\bar{v} + m_+\dot{m}_+ + m_+\dot{m}_+\bar{\rho} + m_+\ddot{m}_+(\bar{t}-t_*) + \frac{m_+^2\ddot{m}_+}{3\bar{v}} \\
&\quad + \frac{\ddot{m}_+}{2}(\bar{t}-t_*)^2\bar{v} + \mathcal{O}(v^{-2})
\end{aligned}
$$

and that

$$
\begin{aligned}
2\mathcal{L}_*^{-1}\tilde{I} &= \tilde{l}\tilde{v} + \tilde{l}\dot{\tilde{l}} + \frac{\tilde{l}^2\ddot{\tilde{l}}}{3\tilde{v}} \\
&= l_-\tilde{v} + l_-\dot{l}_- + l_-\dot{l}_-\tilde{I}(\tilde{\theta} - \theta_2^*) + l_-\ddot{l}_-(\tilde{t}-t_*) + \frac{l_-^2\ddot{l}_-}{3\tilde{v}} \\
&\quad + \frac{\ddot{l}_-}{2}(\tilde{t}-t_*)^2\tilde{v} + \mathcal{O}(v^{-2}).
\end{aligned}
$$

We also note from Equation (3.4) that

$$\tilde{v} = -\bar{v} - 2\dot{m}_+ - 2\ddot{m}_+(\bar{t} - t_*) + \mathcal{O}(v^{-2})$$

and that

$$\begin{aligned}
\bar{t} - \tilde{t} &= \frac{h(\bar{t}) - h(\tilde{t})}{\tilde{v}} = \frac{-m(\bar{t}) + l(\tilde{t}) - 1}{\tilde{v}} \\
&= \frac{-m_+ + l_- - 1}{\tilde{v}} + (-\dot{m}_+ + \dot{l}_-)\frac{\bar{t} - t_*}{\tilde{v}} - \dot{l}_-\frac{\bar{t} - \tilde{t}}{\tilde{v}} + \mathcal{O}(v^{-3}) \\
&= \frac{-m_+ + l_- - 1}{\tilde{v}} + (-\dot{m}_+ + \dot{l}_-)\frac{\bar{t} - t_*}{\tilde{v}} + \dot{l}_-\frac{m_+ - l_- + 1}{\tilde{v}^2} + \mathcal{O}(v^{-3}).
\end{aligned}$$

Therefore

$$\begin{aligned}
2\mathcal{L}_*^{-1}\tilde{I} = &-l_-\bar{v} - 2l_-\dot{m}_+ + m_+\dot{l}_- + m_+\dot{l}_-\bar{\rho} + \dot{l}_- \\
&+ (m_+\ddot{l}_- - 2l_-\ddot{m}_+ + \ddot{l}_-)(\bar{t} - t_*) - \frac{\dddot{l}_-}{2}(\bar{t} - t_*)^2\bar{v} \\
&- \frac{\dddot{l}_-}{2\bar{v}}\left((m_+ + 1)^2 - \frac{l_-^2}{3}\right) + \mathcal{O}(v^{-2})
\end{aligned}$$

hence

$$\begin{aligned}
\frac{2l_-}{\mathcal{M}_*}\bar{J} + \frac{2m_+}{\mathcal{L}_*}\tilde{I} = &\, m_+\dot{l}_- + m_+(l_-\dot{m}_+ - m_+\dot{l}_-)(\bar{\rho} - 1) - \frac{1}{2}\mathcal{L}_* l_- m_+^2\ddot{l}_-\frac{\bar{\rho} - 1}{I} \\
&- \frac{1}{4}\mathcal{L}_* l_- m_+^2(l_-\ddot{m}_+ - m_+\ddot{l}_-)\frac{(\bar{\rho} - 1)^2}{I} \\
&- \frac{1}{12I}\mathcal{L}_* l_- m_+(l_-^2\dddot{l}_- - l_- m_+\dddot{m}_+ - 3\dddot{l}_-) + \mathcal{O}(v^{-2})
\end{aligned}$$

which produces the desired formula together with Lemma 3.2.1. □

3.2.2.4 The Lower-Upper Chamber Case

Finally we suppose that $(\tilde{t}, \tilde{v}) \in \tilde{R}$ and that the ball is in the lower chamber. Also we assume that the next wall is below the previous one when the ball passes through the singularity at $t = t_*$: $h(t_*-) > h(t_*+)$. Also we denote $(\bar{t}, \bar{v}) = H(\tilde{t}, \tilde{v})$.

If $-\tilde{v}(t_* - \tilde{t}) > h(\tilde{t}) + h(t_*-)$, then the ball collides with the floor and enters the upper chamber (c.f. Figure 3.3 on the left).

The imaginary stationary wall trick also applies in this case, which produces a desired formula with the following constants

$$\begin{aligned}
\chi_{Ii} &= \frac{1}{2} l_+ (\dot{l}_+ - l_+ \dot{m}_- / m_-) \\
\chi'_{Ii} &= \frac{1}{2} l_+ \dot{m}_- / m_- \\
\chi''_{Ii} &= \frac{1}{8} l_+ \ddot{m}_- (1 - \frac{1}{3} m_-^2) \\
\chi'''_{Ii} &= \frac{1}{4} l_+^2 (\frac{1}{6} m_- \dddot{l}_+ - \dddot{m}_-) \\
\chi''''_{Ii} &= \frac{1}{8} l_+^3 \dddot{m}_- \\
\chi'''''_{Ii} &= \frac{1}{8} l_+^2 \ddot{l}_+ m_-
\end{aligned}$$

where i indicates that $l(t)$ and $m(t)$ are evaluated at $t = t_i^*$ $(i = 1, 2)$.

Proposition 3.2.7 (Lower-Upper I)**.** *Assume that* $(\rho_1, \mathcal{J}_1) \in R_1^-$ *with* $\mathcal{J}_1 > V_*$ *and that* $-m_2^- \{\mathcal{M}_* \mathcal{J}_1 (\zeta_2^* - \zeta_1^*) - \rho_1\}_2 \gtrsim h(t_2^*-) + h(t_2^*+)$*. Then the Poincaré map* $P_{LU\mathrm{I}}^{12} : R_1^- \to R_2^+$ *is given by*

$$(\bar{\tau}_2, \bar{\mathcal{I}}_2) = G_{LU\mathrm{I}}^{12}(\rho_1, \mathcal{J}_1) + H_{LU\mathrm{I}}^{12}(\rho_1, \mathcal{J}_1) + \mathcal{O}(\mathcal{J}_1^{-2})$$

where

$$G^{12}_{LU\mathrm{I}}(\rho_1,\mathcal{J}_1)=\left(\frac{m_2^-}{l_2^+}\{\mathcal{M}_*\mathcal{J}_1(\zeta_2^*-\zeta_1^*)-\rho_1\}_2+\frac{l_2^+-m_2^-+1}{l_2^+},\right.$$
$$\left.-\frac{l_2^+}{m_2^-}\mathcal{J}_1+\chi_{I2}(\bar\tau_2-1)+\chi'_{I2}\right)$$

and

$$H^{12}_{LU\mathrm{I}}(\rho_1,\mathcal{J}_1)=\left(0,\frac{\chi''_{I2}}{\mathcal{J}_1}+\chi'''_{I2}\frac{\bar\tau_2-1}{\mathcal{J}_1}+\chi''''_{I2}\frac{(\bar\tau_2-1)^2}{\mathcal{J}_1}-\chi'''''_{I2}\frac{(\bar\tau_2-1)^3}{\mathcal{J}_1}\right).$$

Similarly, assume that $(\rho_2,\mathcal{J}_2)\in R_2^-$ *with* $\mathcal{J}_2>V_*$ *and that*

$$-m_1^-\{\mathcal{M}_*\mathcal{J}_2(2+\zeta_1^*-\zeta_2^*)-\rho_1\}_2\gtrsim h(t_1^*-)+h(t_1^*+).$$

Then the Poincaré map $P^{21}_{LU\mathrm{I}}:R_2^-\to R_1^+$ *is given by*

$$(\bar\tau_1,\bar{\mathcal{I}}_1)=G^{21}_{LU\mathrm{I}}(\rho_2,\mathcal{J}_2)+H^{21}_{LU\mathrm{I}}(\rho_2,\mathcal{J}_2)+\mathcal{O}(\mathcal{J}_2^{-2})$$

where

$$G^{21}_{LU\mathrm{I}}(\rho_2,\mathcal{J}_2)=\left(\frac{m_1^-}{l_1^+}\{\mathcal{M}_*\mathcal{J}_2(2+\zeta_1^*-\zeta_2^*)-\rho_2\}_2+\frac{l_1^+-m_1^-+1}{l_1^+},\right.$$
$$\left.\frac{l_1^+}{m_1^-}\mathcal{J}_2+\chi_{I1}(\bar\tau_1-1)+\chi'_{I1}\right)$$

and

$$H^{21}_{LU\mathrm{I}}(\rho_2, \mathcal{J}_2) = \left(0, \frac{\chi''_{I1}}{\mathcal{J}_2} + \chi'''_{I1}\frac{\bar{\tau}_1 - 1}{\mathcal{J}_2} + \chi''''_{I1}\frac{(\bar{\tau}_1 - 1)^2}{\mathcal{J}_2} - \chi'''''_{I1}\frac{(\bar{\tau}_1 - 1)^3}{\mathcal{J}_2}\right).$$

Next, if $-\tilde{v}(t_* - \tilde{t}) < h(\tilde{t}) - h(t_*-)$, then the ball enters the lower chamber immediately after it leaves the previous slit (c.f. Figure 3.3 on the right).

The computation as we have performed for Proposition 3.2.6 can be reproduced here to present the formula in this case, the proof of which we ergo omit. We will need the following constants

$$\begin{aligned}
\chi''_{\mathrm{IIi}} &= \frac{1}{4} l_+^2 \ddot{m}_- \\
\chi'''_{\mathrm{IIi}} &= \frac{1}{8} l_+^2 (m_- \dddot{l}_+ - l_+ \ddot{m}_-) \\
\chi''''_{\mathrm{IIi}} &= \frac{1}{24} l_+ m_- (m_-^2 \ddot{m}_- - m_- l_+ \ddot{l}_+ - 3\ddot{m}_-)
\end{aligned}$$

where i indicates that $l(t)$ and $m(t)$ are evaluated at $t = t_i^*$ $(i = 1, 2)$.

Proposition 3.2.8 (Lower-Upper II)**.** *Assume that* $(\rho_1, \mathcal{J}_1) \in R_1^-$ *with* $\mathcal{J}_1 > V_*$ *and that* $h(t_2^*-) - h(t_2^*+) \gtrsim -m_2^-\{\mathcal{M}_*\mathcal{J}_1(\zeta_2^* - \zeta_1^*) - \rho_1\}_2$*. Then the Poincaré map* $P^{12}_{LU\mathrm{II}} : R_1^- \to R_2^+$ *is given by*

$$(\bar{\tau}_2, \bar{\mathcal{I}}_2) = G^{12}_{LU\mathrm{II}}(\rho_1, \mathcal{J}_1) + H^{12}_{LU\mathrm{II}}(\rho_1, \mathcal{J}_1) + \mathcal{O}(\mathcal{J}_1^{-2})$$

where

$$G^{12}_{LU\mathrm{II}}(\rho_1,\mathcal{J}_1)=\left(\frac{m_2^-}{l_2^+}\{\mathcal{M}_*\mathcal{J}_1(\zeta_2^*-\zeta_1^*)-\rho_1\}_2+\frac{l_2^+-m_2^--1}{l_2^+},\right.$$
$$\left.-\frac{l_2^+}{m_2^-}\mathcal{J}_1+\chi_{I2}(\bar\tau_2-1)-\chi'_{I2}\right)$$

and

$$H^{12}_{LU\mathrm{II}}(\rho_1,\mathcal{J}_1)=\left(0,\chi''_{\mathrm{II}2}\frac{\bar\tau_2-1}{\mathcal{J}_1}-\chi'''_{\mathrm{II}2}\frac{(\bar\tau_2-1)^2}{\mathcal{J}_1}-\frac{\chi''''_{\mathrm{II}2}}{\mathcal{J}_1}\right).$$

Similarly, assume that $(\rho_2,\mathcal{J}_2)\in R_2^-$ *with* $\mathcal{J}_2>V_*$ *and that*

$$h(t_1^*-)-h(t_1^*+)\gtrsim -m_1^-\{\mathcal{M}_*\mathcal{J}_2(2+\zeta_1^*-\zeta_2^*)-\rho_2\}_2.$$

Then the Poincaré map $P^{21}_{LU\mathrm{II}}:R_2^-\to R_1^+$ *is given by*

$$(\bar\tau_1,\bar{\mathcal{I}}_1)=G^{21}_{LU\mathrm{II}}(\rho_2,\mathcal{J}_2)+H^{21}_{LU\mathrm{II}}(\rho_2,\mathcal{J}_2)+\mathcal{O}(\mathcal{J}_2^{-2})$$

where

$$G^{21}_{LU\mathrm{II}}(\rho_2,\mathcal{J}_2)=\left(\frac{m_1^-}{l_1^+}\{\mathcal{M}_*\mathcal{J}_2(2+\zeta_1^*-\zeta_2^*)-\rho_2\}_2+\frac{l_1^+-m_1^--1}{l_1^+},\right.$$
$$\left.-\frac{l_1^+}{m_1^-}\mathcal{J}_2+\chi_{\mathrm{I}1}(\bar\tau_1-1)-\chi'_{\mathrm{I}1}\right)$$

and

$$H^{21}_{LU\mathrm{II}}(\rho_2,\mathcal{J}_2)=\left(0,\chi''_{\mathrm{II}1}\frac{\bar\tau_1-1}{\mathcal{J}_2}-\chi'''_{\mathrm{II}1}\frac{(\bar\tau_1-1)^2}{\mathcal{J}_2}-\frac{\chi''''_{\mathrm{II}1}}{\mathcal{J}_2}\right).$$

3.3 Trapping Regions

In this section, we present the proof of Theorem 1. The assumptions in the theorem lead to the creation of a trapping region where the ball gains energy exponentially fast.

Proof. We choose $V_* \gg 1$ so that the normal forms in Section 3.2.2 hold for $|v| > V_*$. There are two cases.

(i) Suppose that $h_L(t_1^*) < h_R(t_1^*)$ and $h_L(t_2^*) > h_R(t_2^*)$. The relative positions of the two slits at two critical jumps trap the ball forever in the lower region once it enters. Henceforth Proposition 3.2.4 predicts the change of energy after one period in the lower chamber to be

$$\bar{\bar{\mathcal{J}}} = \frac{m_1^+}{m_1^-}\frac{m_2^+}{m_2^-}\mathcal{J} + \mathcal{O}(1)$$

Furthermore, the relative positions of the slits at two critical times guarantee that $m(t_1^*+) < m(t_1^*-) < 0$, $m(t_2^*+) < m(t_2^*-) < 0$, so the energy of the ball grows exponentially fast at rate $\frac{m_1^+}{m_1^-}\frac{m_2^+}{m_2^-} > 1$ in the lower chamber.

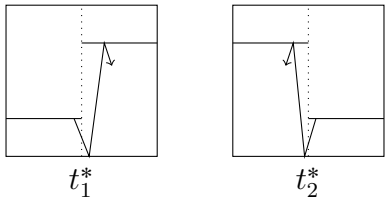

Figure 3.6: The Trapping Lower Chamber

If the ball starts from the lower chamber with $v_0 < -V_*$, it enjoys exponential energy growth with time immediately.

If the ball starts from the upper chamber with $v_0 > V_*$, by Proposition 3.2.3 and the relative positions of the slits, its energy decreases at an exponential rate $\frac{l_1^+}{l_1^-}\frac{l_2^+}{l_2^-} < 1$ until it either enters the lower chamber or it enter the low energy region $|v| < V_*$ where the normal form no longer applies. The possible future when the latter situation occurs is that either the ball remains forever in the low energy region $|v| \leqslant V_*$ or it gets trapped to the lower chamber with some high energy $|v| > V_*$ and then starts exponential acceleration. Now we show that the initial conditions in the upper chamber which leads to bounded orbits contributes a null set.

For any $V > V_*$, we denote

$$\mathcal{U}_V = \{(t_0, v_0) : V < v_0 < V + 1,\ \limsup |v_n| < V_*\}$$

We claim that $\mu(\mathcal{U}_V) = 0$. Otherwise we note that $\mathcal{U}_V \subseteq B_V := \{|v_n| < V + 1,\ \forall n > 0\}$ by the foregoing discussion and B_V is bounded and invariant. Hence, by applying the Poincaré recurrence theorem to (H, μ) on B_V, almost every point in $\mathcal{U}_V$ would return infinitely often to energy level $|v_n| > V$, which contradicts the definition of $\mathcal{U}_V$. Our claim implies that almost all points in the energy shell $\mathcal{W}_V = \{V < v < V + 1\}$ eventually return to some high energy level $|v_n| > V_*$, which is only made possible if the ball enters the lower chamber and Proposition 3.2.4 ensures exponential energy growth afterwards.

(ii) Suppose that $h_L(t_1^*) > h_R(t_1^*)$ and $h_L(t_2^*) < h_R(t_2^*)$. Now the relative positions of the two slits at two critical jumps indicate that the upper region is trapping and then Proposition 3.2.3 guarantees an exponential energy gain at rate

$\frac{l_1^+}{l_1^-}\frac{l_2^+}{l_2^-} > 1$ in the upper chamber once the ball gets trapped. The rest of the analysis is similar to Case (i). □

Example 3.3.1. In general it is not possible to improve the result that non-escaping orbits have finite measure to one with zero measure. For example, we start with $\tilde{h}_L(t) = \tilde{h}_R(t) = a\cos 4\pi t + 0.5$ for some small $a > 0$. We take $x_0 = 0, \lambda = 0.5$, so $t_1^* = 0.5, t_2^* = 1.5$. We consider a 4-periodic orbit $\mathcal{P}$ starting at $t_0 = 0.25, v_0 = 2+4a$. Then

$$(t_1, v_1) = (0.75, 2 + 4a), \quad (t_2, v_2) = (1.25, 2 + 4a), \quad (t_3, v_3) = (1.75, 2 + 4a), \quad .$$

We slightly modify $\tilde{h}_L, \tilde{h}_R$ near t_1^*, t_2^* in such a way that

$$h_L(0.5) > h_R(0.5), \quad h_L(1.5) < h_R(1.5)$$

so that the upper chamber is trapping and that the periodic orbit $\mathcal{P}$ does not see this modification. Observe that $\mathcal{P}$ is elliptic for all small a as the trace of the collision map H along $\mathcal{P}$ is $tr(dH_{\mathcal{P}}) = 2 - \frac{8a\pi^2}{1+2a} \in (0, 2)$ for $0 < a < \frac{1}{4\pi^2-2}$. Now the matrix $dH_{\mathcal{P}}$ is conjugate to a rotation by $2\pi\alpha$ with $\cos 2\pi\alpha = 1 - \frac{4a\pi^2}{1+2a}$. We can easily choose a such that the rotation angle α is Diophantine, then Herman's Last Geometric Theorem guarantees the stability of the elliptic orbit $\mathcal{P}$, i.e. there exists an elliptic island of bounded trajectories around $\mathcal{P}$ (c.f. [16, Theorem 4]).

Although the assumptions of Theorem 1 are compatible with existence of a positive measure set of bounded orbits, we can eliminate the possibility of oscillatory

orbits. Recall that a (forward) oscillatory orbit is an orbit such that

$$\limsup_{t\to+\infty} |v(t)| = \infty \quad \text{and} \quad \liminf_{t\to+\infty} |v(t)| < \infty.$$

Corollary 11. *In presence of a trapping region oscillatory orbits do not exist.*

Proof. We may assume without loss of generality that the lower chamber is trapping. All the high energy orbits in the lower chamber gain energy exponentially immediately.

Now suppose that the ball is in the upper chamber and arrives at high energy level at some $v > V_*$, then it decelerates exponentially as observed in the proof of Theorem 1 until it enters the lower chambers or the normal form no longer applies. In either case, the ball either starts to accelerate exponentially or remains in the low energy region $|v| < V_*$ afterwards. □

3.4 Waiting Time for Exponential Acceleration

In this section we show that in the presence of the trapping region, the majority of orbits with sufficiently high energy get trapped quickly under the hyperbolicity assumption. Throughout this section we assume without loss of generality that the lower chamber is trapping and $|Tr| > 2$. The quantity Tr is in fact the trace of the derivative of the linear map $G_U = G^{21}_{UU} \circ G^{12}_{UU}$ and the hyperbolicity assumption $|Tr| > 2$ indicates that G_U is hyperbolic.

3.4.1 Almost Sure Escape for the Limiting Map

We first restrict ourselves to the linear parts G_{UU}'s of the dynamics in Proposition 3.2.3, which approximates P_{UU}'s with an error of order $\mathcal{O}(I^{-1})$ when the velocity is large $v > V_*$.

We note that

$$\begin{aligned}(\bar{\tau}_2, \bar{I}_2) &= G^{12}_{UU}(\tau_1, I_1) \\ &= \left(-\frac{l_2^-}{l_2^+}\{\mathcal{L}_*\mathcal{I}_1(\theta_2^* - \theta_1^*) - \tau_1\}_2 + 1 + \frac{l_2^-}{l_2^+}, \frac{l_2^+}{l_2^-}\mathcal{I}_1 + \Delta_2(\bar{\tau}_2 - 1) \right)\end{aligned}$$

if $1 - \frac{l_2^+}{l_2^-} < \{\mathcal{L}_*\mathcal{I}_1(\theta_2^* - \theta_1^*) - \tau_1\}_2 < 1 + \frac{l_2^+}{l_2^-}$. The boundary lines

$$\{\mathcal{L}_*\mathcal{I}_1(\theta_2^* - \theta_1^*) - \tau_1\}_2 = 1 - \frac{l_2^+}{l_2^-}, \quad \{\mathcal{L}_*\mathcal{I}_1(\theta_2^* - \theta_1^*) - \tau_1\}_2 = 1 + \frac{l_2^+}{l_2^-} \tag{3.8}$$

cut out from R_1^+ a sequence of boxes

$$A_n = \{1 - \frac{l_2^+}{l_2^-} + 2n < \mathcal{L}_*\mathcal{I}_1(\theta_2^* - \theta_1^*) - \tau_1 < 1 + \frac{l_2^+}{l_2^-} + 2n\}$$

whose points will remain in the upper chamber under G^{12}_{UU}, while the other points will enter the lower chamber, when jumping from right to left at t_2^*.

We also observe that

$$(\bar{\tau}_1, \bar{I}_1) = G^{21}_{UU}(\tau_2, I_2)$$
$$= \left(-\frac{l_1^-}{l_1^+}\{\mathcal{L}_*\mathcal{I}_2(2+\theta_1^*-\theta_2^*)-\tau_2\}_2 + 1 + \frac{l_1^-}{l_1^+}, \frac{l_1^+}{l_1^-}\mathcal{I}_2 + \Delta_1(\bar{\tau}_1 - 1)\right)$$

if $1 - \frac{l_1^+}{l_1^-} < \{\mathcal{L}_*\mathcal{I}_2(2+\theta_1^*-\theta_2^*)-\tau_2\}_2 < 1 + \frac{l_1^+}{l_1^-}$ and that the boundary lines

$$\{\mathcal{L}_*\mathcal{I}_2(2+\theta_1^*-\theta_2^*)-\tau_2\}_2 = 1 - \frac{l_1^+}{l_1^-}, \quad \{\mathcal{L}_*\mathcal{I}_2(2+\theta_1^*-\theta_2^*)-\tau_2\}_2 = 1 + \frac{l_1^+}{l_1^-} \quad (3.9)$$

cut out from R_2^+ another sequence of boxes

$$B_n = \{1 - \frac{l_1^+}{l_1^-} + 2n < \mathcal{L}_*\mathcal{I}_2(2+\theta_1^*-\theta_2^*)-\tau_2 < 1 + \frac{l_1^+}{l_1^-} + 2n\}$$

whose points will remain in the upper chamber under G^{21}_{UU}, while the points outside will enter the lower chamber, when jumping from left to right at t_1^*.

We define $G_U = G^{21}_{UU} \circ G^{12}_{UU}$ on R_1^+. Both G^{12}_{UU} and G^{21}_{UU} are piecewise affine maps, and the derivative of G_U is a constant matrix $DG_U = DG^{21}_{UU} \cdot DG^{12}_{UU}$ where

$$DG^{12}_{UU} = \begin{pmatrix} \frac{l_2^-}{l_2^+} & -\frac{l_2^-}{l_2^+}\mathcal{L}_*(\theta_2^*-\theta_1^*) \\ \Delta_2\frac{l_2^-}{l_2^+} & -\Delta_2\frac{l_2^-}{l_2^+}\mathcal{L}_*(\theta_2^*-\theta_1^*) + \frac{l_2^+}{l_2^-} \end{pmatrix},$$

$$DG^{21}_{UU} = \begin{pmatrix} \frac{l_1^-}{l_1^+} & -\frac{l_1^-}{l_1^+}\mathcal{L}_*(2+\theta_1^*-\theta_2^*) \\ \Delta_1\frac{l_1^-}{l_1^+} & -\Delta_1\frac{l_1^-}{l_1^+}\mathcal{L}_*(2+\theta_1^*-\theta_2^*) + \frac{l_1^+}{l_1^-} \end{pmatrix}$$

Since $\det(DG_U) = 1$ and $|Tr(DG_U)| > 2$, it has unstable eigenvalue Λ_u with

unstable eigenvector $\boldsymbol{e}_u$, and stable eigenvalue Λ_s with stable eigenvector $\boldsymbol{e}_s$.

We observe that each box A is foliated by unstable lines.

We say that an unstable line γ in a box A is *good* if it breaks after one period and at least two components remain in the upper chamber, otherwise we say it is *bad*.

A good line is good as a solid part of it enters the trapping region after one period under the linear map G_U:

Lemma 3.4.1. *Let γ be a good unstable line in some box A. Then the proportion of points on γ which remain in the upper chamber after one period is at most*

$$D = \frac{1 + 2\frac{l_1^+}{l_1^-}}{2 + \frac{l_1^+}{l_1^-}} < 1.$$

Proof. We first note that $G_{UU}^{12}(\gamma)$ remains a complete piece in R_2 as γ lies in A and that G_{UU}^{12} maps the boundaries of A into two vertical lines

$$G_{UU}^{12}\left(\{\mathcal{L}_*\mathcal{I}_1(\theta_2^* - \theta_1^*) - \tau_1\}_2 = 1 - \frac{l_2^+}{l_2^-}\right) \subseteq \{\tau_2 = 2\},$$

$$G_{UU}^{12}\left(\{\mathcal{L}_*\mathcal{I}_1(\theta_2^* - \theta_1^*) - \tau_1\}_2 = 1 + \frac{l_2^+}{l_2^-}\right) \subseteq \{\tau_2 = 0\}.$$

$G_{UU}^{12}(\gamma)$ has to stretch across at least two B-boxes if γ has at least two pieces remaining in the upper chamber after one period.

Suppose that $G_{UU}^{12}(\gamma)$ stretches across N B-boxes for some $N > 1$. It is easy to see that for a fixed N, the highest proportion of points staying in the upper chamber is achieved when $G_{UU}^{12}(\gamma)$ ends on the boundaries of the top and bottom

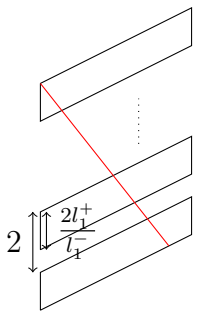

Figure 3.7: A good curve partly enters the trapping region

boxes as shown in Figure 3.7. However the height of a B-box is equal to $2\frac{l_1^+}{l_1^-}$ (c.f. (3.9)) while the height of the fundamental domain is equal to 2 (c.f. Figure 3.7). This implies that in the optimal situation $\frac{2(1-\frac{l_1^+}{l_1^-})(N-1)}{2N+2\frac{l_1^+}{l_1^-}}$ of the points on $G_{UU}^{12}(\gamma)$ land in the lower chamber after jumping from left to right at t_1^*. This proportion is larger than $\frac{(1-\frac{l_1^+}{l_1^-})(2-1)}{2+\frac{l_1^+}{l_1^-}}$ as it is an increasing function in N and $N \geqslant 2$. Then the largest portion which remains in the upper chamber is given by $D = \frac{1+2\frac{l_1^+}{l_1^-}}{2+\frac{l_1^+}{l_1^-}}$. Recall that the relative positions of two slits at t_1^* implies that $\frac{l_1^+}{l_1^-} < 1$, so $D < 1$. □

Next we need to control the number of the short bad pieces as an unstable line breaks under the iterations of the linear map G_U.

Suppose γ is an unstable line in some box A. For $x \in \gamma$, we denote as $r_n(x)$ the distance from x_n to the nearest boundary of the component γ_n containing x_n. Employing the argument in Section 5 of [10] we obtain the following Growth Lemma.

Lemma 3.4.2 (Growth Lemma)**.** *There exists a constant C^* s.t. for any small $\epsilon > 0$ and any $n \in \mathbb{N}$*

$$\text{mes}_\gamma\{x \in \gamma : r_n(x) < \epsilon\} \leqslant C^*\epsilon$$

Proof. Let $k_n(\delta)$ denote the max number of the pieces that an unstable line of length

less than δ can be cut into after n iterates. We define $k_n = \lim_{\delta \to 0} k_n(\delta)$. We claim that $k_n \leqslant 8n$. Indeed since the singularities of G_U^n are lines and there are at most $8n$ possibilities for slopes. Consequently, there exists δ_0 so small that $k_n(\delta) \leqslant 16n$ for any $\delta < \delta_0$. We choose n_0 such that $\frac{32n_0}{\Lambda_u^{n_0}} < 1$ and by replacing G_U with $G_U^{n_0}$ we can always assume $n_0 = 1$.

For inductive purposes we cut a long unstable line into pieces shorter than δ_0 and let $\bar{r}_n(x)$ denote the distance from x_n to the nearest real or artificial boundary of the component containing x_n. We note that by doing so we improve the estimate as $\bar{r}_n(x) \leqslant r_n(x)$ and it suffices to prove the statement for $\bar{r}_n$.

First we observe that

$$\text{mes}_\gamma\{\bar{r}_0(x) < \epsilon\} \leqslant \frac{2L}{\delta_0}\epsilon. \tag{3.10}$$

where L is the unstable height of γ.

$\bar{r}_{n+1}(x)$ is less than ϵ if x_{n+1} either passes a real or artificial singularity. The former is controlled by $2k_1(\delta_0)\text{mes}_\gamma\{r_n < \frac{\epsilon}{\Lambda_u}\}$ while the latter by $\frac{2\epsilon}{\delta_0}$. Therefore

$$\text{mes}_\gamma\{\bar{r}_{n+1} < \epsilon\} \leqslant 32\text{mes}_\gamma\{r_n < \frac{\epsilon}{\Lambda_u}\} + \frac{2\epsilon}{\delta_0}.$$

Thus by induction we conclude that

$$\begin{aligned}\text{mes}_\gamma\{\bar{r}_n < \epsilon\} &\leqslant 32^n \text{mes}_w\left\{\bar{r}_0 < \frac{\epsilon}{\Lambda_u^n}\right\} + \frac{2\epsilon}{\delta_0}\left(1 + \frac{32}{\Lambda_u} + \cdots + \left(\frac{32}{\Lambda_u}\right)^n\right) \\ &\leqslant \left(\frac{32}{\Lambda_u}\right)^n \text{mes}_\gamma\{\bar{r}_0(x) < \epsilon\} + \frac{2\epsilon}{\delta_0}\frac{1}{1 - 32/\Lambda_u}\end{aligned}$$

as $\frac{32}{\Lambda_u} < 1$,. Thus we obtain from (3.10) the desired growth control with

$$C^* = \frac{2L}{\delta_0} + \frac{2}{\delta_0(1 - 32/\Lambda_u)}.$$

□

Finally we show that under the linear approximation map G_U almost every point will eventually escape to the trapping region:

Proposition 3.4.3. *In each box A, for any $\epsilon > 0$, there exists $N = N(\epsilon)$ such that all but an ϵ-measure set of points in A enter the lower chamber within N periods. In particular, almost every point will leave the upper chamber in the future.*

Proof. Fix $\epsilon > 0$. Choose k, l such that

$$D^k L < 0.5\epsilon \quad \text{and} \quad (kl+1)\frac{C^* + L^2}{\Lambda_u^{l/2}} < 0.5\epsilon,$$

and take $N = kl + 1$.

We suppose that under the linear map G_U a point x on a unstable line γ stays in the upper chamber up to N periods.

If the trajectory of x lands on good lines more than k times in N periods, then Lemma 3.4.1 shows that for good lines the portion which remains in the upper chamber in the next period is at most D. Hence by induction we see that

$$\text{mes}_\gamma\{x \in \gamma : \{P_U^m x\}_{m=0}^N \text{ visits good lines more than } k \text{ times}\} < D^k L$$

If instead the trajectory of x visits good lines less than k times in N periods, then it has to visit consecutively l bad lines at least once in N periods.

Now suppose that the trajectory segment $x_n, \cdots, x_{n+l}$ land on bad lines $\gamma_n, \cdots, \gamma_{n+l}$ for some $n < N$ and we denote as $\mathcal{B}_n$ the set of all such $x \in \gamma$ that lands badly during n to $n+l$ periods. We subdivide $\mathcal{B}_n$ into $\mathcal{B}_{n,L}$ and $\mathcal{B}_{n,S}$, where $\mathcal{B}_{n,L}$ collects points with $|\gamma_n| \geqslant \Lambda_u^{-l/2}$ and $\mathcal{B}_{n,S}$ collects points with $|\gamma_n| < \Lambda_u^{-l/2}$.

By Lemma 3.4.2, $|\mathcal{B}_{n,S}| \leqslant C^* \Lambda_u^{-l/2}$. On the other hand, it follows from uniform hyperbolicity that

$$\mathbb{P}_{\gamma_n}\{x_n \text{ returns badly for next } l \text{ periods}\} = \frac{|\gamma_{n+l}|}{\Lambda_u^l |\gamma_n|} \leqslant \frac{L}{\Lambda_u^{l/2}}.$$

Hence

$$|\mathcal{B}_{n,L}| \leqslant \frac{L}{\Lambda_u^{l/2}} \sum_{|\gamma_n| \geqslant \Lambda_u^{-l/2}} |G_U^{-n} \gamma_n| \leqslant \frac{L}{\Lambda_u^{l/2}} |\gamma| \leqslant \frac{L^2}{\Lambda_u^{l/2}}.$$

Combining the estimates on $\mathcal{B}_{n,L}$ and $\mathcal{B}_{n,S}$, we have

$$|\mathcal{B}_n| \leqslant \frac{C^*}{\Lambda_u^{l/2}} + \frac{L^2}{\Lambda_u^{l/2}} = \frac{C^* + L^2}{\Lambda_u^{l/2}}.$$

Consequently the set $\mathcal{B}$ of points on γ which make l consecutive bad landings is controlled in size by

$$|\mathcal{B}| \leqslant (kl+1) \frac{C^* + L^2}{\Lambda_u^{l/2}}.$$

Since a box A is foliated by unstable lines, we conclude by a disintegration of measure argument and our choice of k, l that under the linear map G_U the set of

points in A which stay in the upper chamber for at least N periods has measure less than ϵ. $\square$

3.4.2 Quick Escape for the Actual Map.

By Proposition 3.2.3, the fundamental domains of P_{UU} are $\mathcal{O}(\mathcal{I}^{-1})$-deformation of the boxes A, B and $P_{UU} = G_{UU} + \mathcal{O}(\mathcal{I}^{-1})$.

Now we prove Theorem 2.

Proof of Theorem 2. Fix $\epsilon > 0$ and a box A with large energy $\tilde{\mathcal{I}}_0$ (to be specified later). By Proposition 3.4.3 we choose N such that in each A-box the points that remain in the upper chamber up to N periods under the linear approximation G_U take up a set of measure less than 0.5ϵ, i.e. we take $N = kl+1$ where k, l are integers such that

$$k > \frac{\log(0.25\epsilon/L)}{\log D} \quad \text{and} \quad \frac{kl+1}{\Lambda_u^{l/2}} < \frac{0.25\epsilon}{C^* + L^2}. \tag{3.11}$$

We shall show that the statement of Theorem 2 holds with some large $\tilde{\mathcal{I}}_0 = \tilde{\mathcal{I}}_0(\epsilon)$ and

$$T = 2N. \tag{3.12}$$

Let A_n^δ and B_n^δ denote the points in A_n and B_n which are closer than δ to the boundary,

$$\mathcal{A}^\delta = \bigcup_n A_n^\delta, \quad \widetilde{\mathcal{A}}^\delta = \bigcup_n \left(A_n - \backslash A_n^\delta\right),$$

$$\mathcal{B}^\delta = \bigcup_n B_n^\delta, \quad \widetilde{\mathcal{B}}^\delta = \bigcup_n \left(B_n - \backslash B_n^\delta\right).$$

Choose $\delta < 0.5\epsilon$ so that the set of points in the box A which visit either $\mathcal{A}^\delta$ or $\mathcal{B}^\delta$ during the first N iterations is less than 0.5ϵ.

By Proposition 3.2.3, there is a constant C_1 such that if $P_{UU}^{12}(x) \in \widetilde{\mathcal{B}}^{C_1/\mathcal{I}}$ and $P_{UU}^{21}(P_{UU}^{12}x) \in \widetilde{\mathcal{A}}^{C_1/\mathcal{I}}$ then the orbit of x stays in the upper chamber for the next period and

$$|P_U(x) - G_U(x)| \leqslant \frac{C_1}{\mathcal{I}} \quad \text{where} \quad P_U = P_{UU}^{21} \circ P_{UU}^{12}.$$

Accordingly there is a constant C_2 such that if for some $n \leqslant N$

$$P_{UU}^{12} P_U^k(x) \in \widetilde{\mathcal{B}}^{\frac{C_2 \Lambda_u^N}{\mathcal{I}^*}}, \quad P_U^{k+1}(x) \in \widetilde{\mathcal{A}}^{\frac{C_2 \Lambda_u^N}{\mathcal{I}^*}} \tag{3.13}$$

and $\mathcal{I}_k \geqslant \mathcal{I}^*$ for $k < n$ then the real orbit of x stays in upper chamber for the first n iterations and

$$|P_U^n(x) - G_U^n(x)| \leqslant \frac{C_2 \Lambda_u^N}{\mathcal{I}^*}. \tag{3.14}$$

Next, set $C_3 = \frac{l_2^+ l_1^+}{l_2^- l_1^-} < 1$. Then during N iterations the value of I cannot drop by more than C_3^N times. Hence if x satisfies (3.13) and $\mathcal{I}_0 \geqslant C_3^N \mathcal{I}^*$ then (3.14) holds.

Now choose $\mathcal{I}^*$ so that

$$\frac{C_2 \Lambda_u^N}{\mathcal{I}^*} < \delta \tag{3.15}$$

Now we consider the orbits where $\bar{\mathcal{I}} \leqslant \mathcal{I}_0 \leqslant \bar{\mathcal{I}} + 1$ for some $\bar{\mathcal{I}} \geqslant C_3^N \mathcal{I}^*$. There are three possibilities:

(i) The real orbit of x leaves the upper chamber at some period $n < N$;

(ii) The real orbit of x stays in $\widetilde{\mathcal{A}}^\delta$ for the first N iterations;

(iii) The real orbit of x stays in $\widetilde{\mathcal{A}}^{\delta}$ until it hits $\mathcal{A}^{\delta} \cup (P_U^{12})^{-1}\mathcal{B}^{\delta}$ at some period $n < N$.

Proposition 3.4.3 and our choice of δ and $\mathcal{I}^*$ imply that the set of orbits where either (ii) or (iii) happens has measure smaller than ϵ.

This completes the proof of Theorem 2. □

Chapter 4: Bouncing Ball in a Gravity Field

In this Chapter, we present the proofs of the Theorems stated in Section 2.2.

4.1 Preliminaries

In this section, we discuss the collision map. The study of the collision map relies substantially on the behavior of its limiting map, i.e. the approximated collision map for large velocities. We also discuss the singularity lines/curves of the limit map as they will play a very important role in the proofs later.

4.1.1 The Collision Map

We denote $s_n = t_{n+1} - t_n$ the flight time between two consecutive collisions.

Two consecutive collisions satisfy the following equations

$$\begin{cases} -(v_n - gs_n - \dot{f}(t_{n+1})) = v_{n+1} - \dot{f}(t_{n+1}) \\ f(t_n) + v_n s_n - \dfrac{1}{2} g s_n^2 = f(t_{n+1}). \end{cases} \tag{4.1}$$

We compute the derivative of the collision map F by differentiating these

equations

$$dF = \begin{pmatrix} 1 + \frac{\dot{f}(t_n) - \dot{f}(t_{n+1})}{w_{n+1}} & \frac{s_n}{w_{n+1}} \\ 2\ddot{f}(t_{n+1}) + (2\ddot{f}(t_{n+1}) + g)\frac{\dot{f}(t_n) - \dot{f}(t_{n+1})}{w_{n+1}} & (2\ddot{f}(t_{n+1}) + g)\frac{s_n}{w_{n+1}} - 1 \end{pmatrix}.$$

We observe that $\det dF = \frac{w_n}{w_{n+1}}$ and hence F preserves the measure $\mu = wdtdv$ on the phase cylinder.

4.1.2 The Limit Map

If we only consider collisions with large velocities, the dynamics can be approximated by

$$F(t, v) = F_\infty(t, v) + \mathcal{O}\left(\frac{1}{v}\right)$$

where

$$F_\infty(t, v) = \left(t + \frac{2v}{g}, v + 2\dot{f}\left(t + \frac{2v}{g}\right)\right).$$

Denote as $(t_1, v_1) = F_\infty(t_0, v_0)$, then

$$t_1 = t_0 + \frac{2v_0}{g}, \quad v_1 = v_0 + 2\dot{f}(t_1).$$

As mentioned in Section 2.2, the limit map F_∞ covers a map $\tilde{F}_\infty$ on the torus $\mathbb{T} = \mathbb{R}/\mathbb{Z} \times \mathbb{R}/g\mathbb{Z}$

$$\tilde{t}_1 = \tilde{t}_0 + \frac{2\tilde{v}_0}{g}, \ \tilde{v}_1 = \tilde{v}_0 + 2\dot{f}(\tilde{t}_1)$$

where $\tilde{t} = t \pmod 1$, $\tilde{v} = v \pmod g$.

Denote as $k(t) = \ddot{f}(t)$. The dynamics of $\tilde{F}_\infty$ can be decomposed as

$$\tilde{t}_1 = \tilde{t}_0 + \frac{2\tilde{v}_0}{g} \pmod 1,\ \tilde{v}_0 = \tilde{v}_0,$$

and

$$\tilde{t}_1 = \tilde{t}_1,\ \tilde{v}_1 = \tilde{v}_0 + 2\dot{f}(\tilde{t}_1).$$

Hence the derivative of $\tilde{F}_\infty$ at $(\tilde{t}_0, \tilde{v}_0)$ is

$$d_{(\tilde{t}_0,\tilde{v}_0)}\tilde{F}_\infty = \begin{pmatrix} 1 & \frac{2}{g} \\ 2k_1 & \frac{4k_1}{g} + 1 \end{pmatrix}.$$

We observe that $\det d\tilde{F}_\infty = 1$, so $\tilde{F}_\infty$ preserves the Lebesgue measure $\tilde{\mu} = d\tilde{t}d\tilde{v}$ on the torus.

4.1.3 The Singularity Lines of the Limit Map

A singularity occurs when the ball collides with wall at the singularities of the wall motion, i.e. $t \in \mathbb{N}$, hence the singularity line $\mathcal{S}^+$ of $\tilde{F}_\infty$ consists of the points whose next collisions happen at integer times, i.e.

$$\mathcal{S}^+ = \{\tilde{t}_1 = 0\} = \left\{\tilde{t}_0 + \frac{2\tilde{v}_0}{g} \equiv_1 0\right\}.$$

Similarly, the singularity line $\mathcal{S}^-$ of $\tilde{F}_\infty^{-1}$ consists of the points whose the preimages land on integer times, i.e.

$$\mathcal{S}^- = \{\tilde{t}_{-1} = 0\} = \left\{\tilde{t}_0 + \frac{4}{g}\dot{f}(\tilde{t}_0) - \frac{2\tilde{v}_0}{g} \equiv_1 0\right\}.$$

We observe that $\mathcal{S}^\pm$ consists of finitely many line/curve segments.

4.2 Ergodicity of the Limit Map

In this section we establish the ergodicity of the limit map $\tilde{F}_\infty$ under the assumptions in Theorem 3 and Theorem 4. We use the result by Liverani and Wojtkowski in [30] where they proved ergodicity for a large class of Hamiltonian systems with invariant cones. We first describe the class of symplectic maps (X, T) considered in [30] and then show that $\tilde{F}_\infty$ satisfies the conditions of [30].

Those conditions involve strictly invariant cones and the least coefficient of expansion, which are defined as follows. Suppose (X, ω) is a compact symplectic manifold and $T : X \circlearrowleft$ is a symplectic map preserving ω. For a point $p \in X$, let V_1^p and V_2^p be two transverse Lagrangian subspaces of T_pX, then each vector $v \in T_pX$ has unique decomposition $v = v_1 + v_2$ with $v_i \in V_i^p$. For any $p \in X$, we define the following quadratic form $\mathcal{Q}_p(v) = \omega(v_1, v_2)$ where $v = v_1 + v_2 \in T_pX$ is the decomposition mentioned before. For any $p \in X$, we consider these two complementary cones

$$\mathcal{C}(p) = \{v \in T_pX : \mathcal{Q}_p(v) \geqslant 0\}, \quad \mathcal{C}'(p) = \{v \in T_pX : \mathcal{Q}_p(v) \leqslant 0\}.$$

We say p possesses *strictly monotone cones* if d_pT preserves strictly $\mathcal{C}(p)$ and d_pT^{-1} preserves strictly $\mathcal{C}'(p)$.

For $p \in X$ with strictly monotone cones $\mathcal{C}(p), \mathcal{C}'(p)$, the *coefficient β of expansion at* $v \in T_pX$ is defined as

$$\beta(v, d_pT) = \sqrt{\frac{\mathcal{Q}_p(d_pTv)}{\mathcal{Q}_p(v)}}$$

and the *least coefficient σ of expansion* is defined as

$$\sigma(d_pT) = \inf_{v \in int\mathcal{C}(p)} \beta(v, d_pT).$$

Now we list here the six conditions of [30] in two dimensional case.

1. The phase space X is a finite disjoint union of compact subsets of a linear symplectic space $\mathbb{R}^2$ with dense and connected interior and *regular* boundaries, i.e. they are finite unions of curves which intersect each other at at most finitely many points.

2. For every $n \geqslant 1$ the singularity sets $\mathcal{S}_n^+$ and $\mathcal{S}_n^-$ of T^n and T^{-n} respectively are regular.

3. Almost every point $p \in X$ possesses strictly monotone cones $\mathcal{C}(p)$ and its complementary $\mathcal{C}'(p)$.

4. The singularity sets $\mathcal{S}^+$ and $\mathcal{S}^-$ are *properly aligned*, i.e. the tangent line of $\mathcal{S}^-$ at any $p \in \mathcal{S}^-$ is contained strictly in the cone $\mathcal{C}(p)$ and the tangent line of $\mathcal{S}^+$ at any $p \in \mathcal{S}^+$ is contained strictly in the complementary cone $\mathcal{C}'(p)$. In

fact, it is sufficient to assume that there exists N such that $T^N\mathcal{S}^-$ and $T^{-N}\mathcal{S}^+$ are properly aligned.

5. *Noncontraction*: There is a constant $a \in (0,1]$ such that for every $n \geqslant 1$ and for every $p \in X \backslash \mathcal{S}_n^+$

$$||d_pT^n v|| \geqslant a||v||$$

for every vector $v \in \mathcal{C}(p)$.

6. *Sinai-Chernov Ansatz*: For almost every $p \in \mathcal{S}^-$ with respect to the measure $\mu_{\mathcal{S}}$, its least coefficient of expansion satisfies

$$\lim_{n\to\infty} \sigma(d_pT^n) = \infty.$$

We note from [30] that σ is supermultiplicative, i.e. $\sigma(d_{Tp}Td_pT) \geqslant \sigma(d_{Tp}T)\sigma(d_pT)$, and that if the coordinates are such that the cone $\mathcal{C}(p)$ is the positive cone (i.e. $\mathcal{C}(p) = \{\delta x \delta y \geqslant 0\}$) and d_pT takes the form

$$d_pT = \begin{pmatrix} A_p & B_p \\ C_p & D_p \end{pmatrix},$$

then σ can be computed as $\sigma(d_pT) = \sqrt{1+t_p} + \sqrt{t_p}$ where $t_p = B_pC_p$.

Liverani and Wojtkowski have proved local ergodicity for symplectic maps satisfying the above six conditions:

Theorem 12 ([30]). *Suppose (X,T) satisfies the above conditions. For any $n \geqslant 1$*

and for any $p \in X \backslash \mathcal{S}_n^+$ such that $\sigma(d_p T^n) > 3$ there is a neighborhood of p which is contained in one ergodic component of T.

Now we prove Theorem 3:

Proof of Theorem 1. Suppose that $\ddot{f} > 0$.

First we prove local ergodicity by verifying the above six conditions for $\tilde{F}_\infty$.

The singularity lines $\mathcal{S}^\pm$ are finite unions of short lines/curves and they cut our phase space X, which is a torus, into finitely many pieces.

The strict monotonicity follows easily from the fact that $d\tilde{F}_\infty$ is positive when $\ddot{f} > 0$, hence $d_p\tilde{F}_\infty$ preserves strictly the positive cone $\mathcal{C}^+(p) = \{\delta\tilde{t}\delta\tilde{v} \geqslant 0\}$ and $d_p\tilde{F}_\infty^{-1}$ preserves strictly the complementary negative cone $\mathcal{C}^-(p) = \{\delta\tilde{t}\delta\tilde{v} \leqslant 0\}$.

It is straightforward from the previous discussion that $\mathcal{S}^\pm$ are properly aligned since the slope of tangent line to $\{\tilde{t}_1 = 0\}$ at $(\tilde{t}_0, \tilde{v}_0)$ is $-\dfrac{g}{2} < 0$, and the slope of the tangent line to $\{\tilde{t}_{-1} = 0\}$ is $\dfrac{g}{2}\left(1 + \dfrac{4k_0}{g}\right) > 0$.

Next we verify the noncontraction property.

For any nonsingular point $p = (\tilde{t}, \tilde{v})$, any vector $\boldsymbol{v} = (\delta\tilde{t}, \delta\tilde{v}) \in \mathcal{C}^+(p)$ with $\delta\tilde{t}\delta\tilde{v} \geqslant 0$,

$$\begin{aligned} ||d_p\tilde{F}_\infty \boldsymbol{v}||^2 &= (1 + 4k_1^2)\delta\tilde{t}^2 + \left(\frac{4}{g^2} + \left(\frac{4k_1}{g} + 1\right)^2\right)\delta\tilde{v}^2 + \left(\frac{4}{g} + 4k_1\left(\frac{4k_1}{g} + 1\right)\right)\delta\tilde{t}\delta\tilde{v} \\ &\geqslant \delta\tilde{t}^2 + \delta\tilde{v}^2 = ||\boldsymbol{v}||^2 \end{aligned} \tag{4.2}$$

thus the noncontraction property follows for $a = 1$.

Now we verify the Sinai-Chernov Ansatz.

We denote as $\mathcal{S}_0 = \{\tilde{t}_0 = 0\}$. For any point $p \in \mathcal{S}^- \setminus \cup_{n\geqslant 0} \mathcal{S}_n$, which excludes a $\tilde{\mu}_{\mathcal{S}^-}$-null set since $\mathcal{S}^-$ intersect each $\mathcal{S}_n$ at at most finitely many points,

$$\sigma(d_p\tilde{F}_\infty) = \sqrt{1+\frac{4k_1}{g}} + \sqrt{\frac{4k_1}{g}} \geqslant \sqrt{1+\frac{4k_{\min}}{g}} + \sqrt{\frac{4k_{min}}{g}} > 1,$$

where $k_{\min} = \min\limits_{t\in(0,1)} \ddot{f}(t) > 0$ by our assumption, then the supermultiplicativity of σ implies that $\lim\limits_{n\to\infty} \sigma(d_p\tilde{F}_\infty^n) = \infty$.

Finally, it remains to check that the singularity sets $\mathcal{S}_n^-$ and $\mathcal{S}_n^+$ of $\tilde{F}_\infty^n$ and $\tilde{F}_\infty^{-n}$ respectively are regular. We claim that for every $n > 0$, $\mathcal{S}_n^-$ ($\mathcal{S}_n^+$) is a finite union of increasing (decreasing) curves, i.e. curves with bounded positive (negative) slope. This can be proved by an inductive argument. Firstly the claim holds for $n = 1$ as already shown before. Now suppose $\mathcal{S}_n^-$ is a finite union of increasing curves. Since $\mathcal{S}_{n+1}^- = \mathcal{S}_n^- \cup \tilde{F}_\infty\mathcal{S}_n^-$ and $d\tilde{F}_\infty$ is a positive matrix and the second derivative $\ddot{f}$ is bounded, $\mathcal{S}_{n+1}^-$ is a finite union of increasing curves. The claim for $\mathcal{S}_n^+$ can be proved similarly.

Observe that $k(t) = \ddot{f}(t) > 0$ is uniformly bounded, hence there exists $N > 0$ such that $\sigma(d_p\tilde{F}_\infty^N) > 3$ for any $p \notin \mathcal{S}_N^+$. Therefore we have obtained local ergodicity for $\tilde{F}_\infty$ by Theorem 12.

Now we argue for global ergodicity by contradiction.

Suppose that there exists some nontrivial ergodic component M of $\tilde{F}_\infty$, then its boundary ∂M lies on $\mathcal{S}_N^+$. But

$$\mathcal{S}_N^+ = \bigcup_{n=0}^{N-1} \tilde{F}_\infty^{-n}\mathcal{S}^+$$

hence there exists a smallest integer $N_0 \geqslant 1$ such that $\partial M \in \mathcal{S}^+_{N_0}$.

Observe that $\tilde{F}_\infty(\partial M) = \partial M$ by the invariance of M. However, $\tilde{F}_\infty(\mathcal{S}^+_{N_0}) = \mathcal{S}^+_{N_0-1} \cup \mathcal{S}_0$, which contradicts the minimality of N_0. Note that although $\tilde{F}_\infty$ is multivalued at $\mathcal{S}^+$, we have $\tilde{F}_\infty \mathcal{S}^+ = \mathcal{S}_0$ anyway.

Therefore we conclude that there cannot be any nontrivial ergodic component and hence $\tilde{F}_\infty$ is ergodic. □

The proof of Theorem 4 follows a similar strategy. The main difficulty arises from finding invariant cones as the derivative matrix is no longer positive. However we still manage to construct invariant cones out of the "eigenvectors" of the derivative matrix.

Proof of Theorem 4. Suppose $\ddot{f} < -g$.

First of all, we recall that the derivative of $\tilde{F}_\infty$ at $(\tilde{t}_0, \tilde{v}_0)$ is

$$d_{(\tilde{t}_0,\tilde{v}_0)}\tilde{F}_\infty = \begin{pmatrix} 1 & \frac{2}{g} \\ 2k_1 & \frac{4k_1}{g} + 1 \end{pmatrix}.$$

Now we consider the following two cones

$$\mathcal{C}^u(\tilde{t}_0, \tilde{v}_0) = \left\{ \frac{\delta v}{\delta t} \leqslant k_0 \right\}, \quad \mathcal{C}^s(\tilde{t}_0, \tilde{v}_0) = \left\{ \frac{\delta v}{\delta t} \geqslant k_0 \right\}$$

We verify that they are invariant under $d_{(\tilde{t}_0,\tilde{v}_0)}\tilde{F}_\infty$ and $d_{(\tilde{t}_0,\tilde{v}_0)}\tilde{F}_\infty^{-1}$ respectively.

For any $(\delta t, \delta v) \in \mathcal{C}^u(\tilde{t}_0, \tilde{v}_0)$,

$$\begin{pmatrix} \bar{\delta t} \\ \bar{\delta v} \end{pmatrix} = \begin{pmatrix} 1 & \frac{2}{g} \\ 2k_1 & \frac{4k_1}{g} + 1 \end{pmatrix} \begin{pmatrix} \delta t \\ \delta v \end{pmatrix} = \begin{pmatrix} \delta t + \frac{2}{g}\delta v \\ 2k_1(\delta t + \frac{2}{g}\delta v) + \delta v \end{pmatrix}$$

thus

$$\begin{aligned} \frac{\bar{\delta v}}{\bar{\delta t}} &= 2k_1 + \frac{\frac{\delta v}{\delta t}}{1 + \frac{2}{g}\frac{\delta v}{\delta t}} \\ &\leqslant 2k_1 + \frac{k_0}{1 + \frac{2k_0}{g}} \\ &< 2k_1 + g < k_1 \end{aligned} \tag{4.3}$$

where the first inequality follows from $\frac{\delta v}{\delta t} \leqslant k_0$ and the last two inequalities from $\ddot{f} < -g$. Thus $(\bar{\delta t}, \bar{\delta v}) \in \mathcal{C}^u(\tilde{t}_1, \tilde{v}_1)$.

For any $(\delta t, \delta v) \in \mathcal{C}^s(\tilde{t}_0, \tilde{v}_0)$

$$\begin{pmatrix} \tilde{\delta t} \\ \tilde{\delta v} \end{pmatrix} = \begin{pmatrix} \frac{4k_0}{g} + 1 & -\frac{2}{g} \\ -2k_0 & 1 \end{pmatrix} \begin{pmatrix} \delta t \\ \delta v \end{pmatrix} = \begin{pmatrix} \delta t - \frac{2}{g}(-2k_0\delta t + \delta v) \\ -2k_0\delta t + \delta v \end{pmatrix},$$

thus

$$\begin{aligned} \frac{\tilde{\delta v}}{\tilde{\delta t}} &= -\frac{g}{2} + \frac{g}{2}\frac{1}{1 + \frac{2}{g}(2k_0 - \frac{\delta v}{\delta t})} \\ &> -\frac{g}{2} + \frac{g}{2}\frac{1}{1 + \frac{2k_0}{g}} \\ &> -g > k_{-1} \end{aligned} \tag{4.4}$$

where the first inequality follows from $\frac{\delta v}{\delta t} \geqslant k_0$ and the last two inequalities from

$\ddot{f} < -g$. Thus $(\tilde{\delta t}, \tilde{\delta v}) \in \mathcal{C}^u(\tilde{t}_{-1}, \tilde{v}_{-1})$.

If we can verify that $\mathcal{S}^{\pm}$ are properly aligned, then the regularity of the singularity curves $\mathcal{S}_n^{\pm}$ follows automatically from the strict invariance of the cones $\mathcal{C}^{u/s}$ since $\mathcal{S}_n^{\pm}$ consist of finitely many transverse short curves.

We claim that $\mathcal{S}^{\pm}$ are properly aligned. Indeed, the slope of tangent line to $\{\tilde{t}_1 = 0\}$ at $(\tilde{t}_0, \tilde{v}_0)$ is $-\frac{g}{2} > k_0$, which is properly contained in $\mathcal{C}^s$. Also, the slope of the tangent line to $\{\tilde{t}_{-1} = 0\}$ is $2k_0 + \frac{g}{2} < k_0$, which is properly contained in $\mathcal{C}^u$.

The noncontraction property still holds with $a = 1$.

The unstable cone $\mathcal{C}^u$ is not canonical, i.e. it is not the positive cone, hence we need to switch to the new basis $((0,1),(1,k_0))$ and $d_p\tilde{F}_\infty$ takes the form

$$\begin{pmatrix} \frac{2k_1}{g} + 1 & k_0 + k_1 + \frac{2k_0k_1}{g} \\ 2/g & 1 + \frac{2k_0}{g} \end{pmatrix}$$

Then the Sinai-Chernov Ansatz holds since

$$\begin{aligned} \sigma(d_p\tilde{F}_\infty) &= \sqrt{1 + \frac{2}{g}\left(\frac{2k_0k_1}{g} + k_0 + k_1\right)} + \sqrt{\frac{2}{g}\left(\frac{2k_0k_1}{g} + k_0 + k_1\right)} \\ &\geqslant \sqrt{1 + \frac{2}{g}\left(\frac{2k_{\min}^2}{g} + 2k_{\min}\right)} + \sqrt{\frac{2}{g}\left(\frac{2k_{\min}^2}{g} + 2k_{\min}\right)} > 1. \end{aligned}$$

By Theorem 12 the local ergodicity of $\tilde{F}_\infty$ holds for the case when $\ddot{f} < -g$. Finally, the global ergodicity can be obtained by a similar argument as in the proof of Theorem 3. □

4.3 Recurrence of the Collision Map

In this section, we prove Theorem 7 and Theorem 8 as they are direct consequences of the ergodicity of the limit map $\tilde{F}_\infty$ on the torus.

The proof of Theorem 7 uses a result from [8], which shows that for an asymptotically periodic map with an ergodic limiting map, if the energy change in the limiting map has zero average, then the escaping orbits of the original dynamics have zero measure.

We state this result for our case specifically. First we decompose the velocity v into integer part and fractional part, i.e. there exists some $m \in \mathbb{Z}$ such that

$$v = \tilde{v} + mg \text{ where } \tilde{v} \in [0, g).$$

Then we decompose the limit map F_∞ on the cylinder into its projection $\tilde{F}_\infty$ on the torus and a map γ on integers $\mathbb{Z}$, i.e.

$$(\tilde{t}_1, \tilde{v}_1, m_1) = F_\infty(\tilde{t}_0, \tilde{v}_0, m_0) = (\tilde{F}_\infty(\tilde{t}_0, \tilde{v}_0), m_0 + \gamma(\tilde{t}_0, \tilde{v}_0)).$$

Lemma 4.3.1 ([8]). *Suppose that $\tilde{F}_\infty$ is ergodic with respect to the measure $\tilde{\mu} = d\tilde{t}d\tilde{v}$ on the torus. If the energy change of F_∞ has zero average, i.e. $\int_{\mathbb{T}} \gamma(\tilde{t}_0, \tilde{v}_0) d\tilde{\mu} = 0$, then the escaping set of F has zero measure.*

Now we prove Theorem 7.

Proof of Theorem 7. If $f(t)$ is admissible, then, by Theorems 3 and 4, $\tilde{F}_\infty$ is ergodic.

Thus by Lemma 4.3.1, it suffices to check that the energy change γ of F_∞ has zero average.

With an abuse of notation, let us denote $(t_1, v_1) = F_\infty(t_0, v_0)$ and $(\tilde{t}_1, \tilde{v}_1) = \tilde{F}_\infty(\tilde{t}_0, \tilde{v}_0)$ respectively. Observe that

$$\int \tilde{v}_0 d\tilde{\mu} = \int \tilde{v}_1 d\tilde{\mu}$$

since $\tilde{F}_\infty$ preserves the measure $\tilde{\mu}$. Thus

$$\int \gamma d\tilde{\mu} = \frac{1}{g} \int (v_1 - v_0) d\tilde{\mu}.$$

But $v_1 - v_0 = 2\dot{f}(\tilde{t}_1)$, hence

$$\int (v_1 - v_0) d\tilde{\mu} = \int 2\dot{f}(\tilde{t}_1) d\tilde{\mu} = \int 2\dot{f}(\tilde{t}_0) d\tilde{\mu} = 0$$

where the last two equalities follow from the fact that $\tilde{F}_\infty$ preserves $\tilde{\mu}$ and that f is 1-periodic. Therefore by Lemma 4.3.1 the escaping orbits of F have zero measure. □

The set E of escaping orbits is in fact the transient part of F, hence Theorem 7 implies that F is recurrent, in the spirit of [10]:

Proof of Corollary 8. We claim that the set E of escaping orbits is the transient component of the system. Hence Theorem 7 implies Corollary 8.

Indeed, the complement of E is $\cup E_N$ where

$$E_N = \{(t_0, v_0) : \liminf v_n \leqslant N\}.$$

For any $N \in \mathbb{N}$, E_N is invariant and all points in E_N will visit the set $V_N = \{v \leqslant N+1\}$.

Suppose A is a subset of E_N with finite measure. For any $x \in A$, we denote the first hitting time in V_N as $r(x) = \min\{k \geqslant 0 : F^k x \in V_N\}$. Now for any $K \in \mathbb{N}$, we consider

$$A_K := \bigcup_{x \in A : r(x) \leqslant K} F^{r(x)} x.$$

To show recurrence in A, it suffices to prove that almost every point in A_K visits itself infinitely often since if for $x \in A_K$ $F^n x \in A_K$ for some $n > K$, then there exists some $x' \in A$ such that $F^{n-r(x')} x = x' \in A$.

However $A_K \subseteq E_N \cap V_N$ by definition of A_K and the invariance of E_N. All points in E_N visit V_N, thus the first return map P on A_K is well-defined. Now our goal is achieved by applying Poincaré recurrence theorem to (A_K, P). □

4.4 Statistical Properties of the Limit Map

In this section we prove Theorem 5, Theorem 6 and Theorem 10. Throughout this section we assume the wall motion is admissible.

4.4.1 Background.

The proof of Theorem 5 uses a result of Chernov and Zhang in [6] and the proof of Theorem 6 uses a result of Chernov in [5]. We first describe the class of hyperbolic symplectic maps considered in [5, 6] and then show that our map $\tilde{F}_\infty$ belongs to this class.

Let $T : M \to M$ be a C^2 diffeomorphism of a two dimensional Riemannian manifold M with singularities $\mathcal{S}$. Suppose T satisfies the following conditions:

1. *Uniform hyperbolicity of T.* There exist two continuous families of unstable cones $\mathcal{C}_x^u$ and stable cones $\mathcal{C}_x^s$ in the tangent spaces $\mathcal{T}_x M$ for all $x \in M$, and $\exists$ a constant $\Lambda > 1$ such that

   (a) $DT(\mathcal{C}_x^u) \subset \mathcal{C}_{Tx}^u$, and $DT(\mathcal{C}_x^s) \supset \mathcal{C}_{Tx}^s$ whenever DT exists;

   (b) $||D_x T\mathrm{v}|| \geqslant \Lambda ||\mathrm{v}|| \ \forall \mathrm{v} \in \mathcal{C}_{\mathrm{x}}^{\mathrm{u}}$, and $||D_x T^{-1}\mathrm{v}|| \geqslant \Lambda ||\mathrm{v}|| \ \forall \mathrm{v} \in \mathcal{C}_{\mathrm{x}}^{\mathrm{s}}$;

   (c) The angle between $\mathcal{C}_x^u$ and $\mathcal{C}_x^s$ is uniformly bounded away from zero.

2. *Singularities $\mathcal{S}^{\pm}$ of T and T^{-1}.* The singularities $\mathcal{S}^{\pm}$ have the following properties:

   (a) $T : M \backslash \mathcal{S}^+ \to M \backslash \mathcal{S}^-$ is a C^2 diffeomorphism;

   (b) $\mathcal{S}_0 \cup \mathcal{S}^+$ is a finite or countable union of smooth compact curves in M;

   (c) Curves in $\mathcal{S}_0$ are transverse to the stable and unstable cones. Every smooth curve in $\mathcal{S}^+$ ($\mathcal{S}^-$) is a stable (unstable) curve. Every curve in $\mathcal{S}^+$ terminates either inside another curve of $\mathcal{S}^+$ or on $\mathcal{S}_0$;

   (d) $\exists\ \beta \in (0,1)$ and $c > 0$ such that for any $x \in M \backslash \mathcal{S}^+$, $||D_x T|| \leqslant c d(x, \mathcal{S}^+)^{-\beta}$.

3. *Regularity of smooth unstable curves.* We assume there exists a T-invariant class of unstable curves W such that

   (a) *Bounded curvature.* The curvature of W is uniformly bounded from above;

(b) *Distortion control.* $\exists\ \gamma \in (0,1)$ and $C > 1$ such that for any regular unstable curve W and any $x, y \in W$

$$\left|\log \mathcal{J}_W(x) - \log \mathcal{J}_W(y)\right| \leqslant C d(x,y)^\gamma,$$

where $\mathcal{J}_W(x) = |D_x T|_W|$ denotes the Jacobian of T at $x \in W$;

(c) *Absolute continuity of the holonomy map.* Let W_1, W_2 be two regular unstable curves that are close to each other. We denote

$$W_i' = \{x \in W_i : W^s(x) \cap W_{3-i} \neq \varnothing\}, \quad i = 1, 2.$$

The holonomy map $h : W_1' \to W_2'$ is defined by sliding along the stable manifold. We assume that $h_\star \mu_{W_1'} \ll \mu_{W_2'}$ and that for some constant C and $\vartheta < 1$

$$\left|\log \mathcal{J}h(x) - \log \mathcal{J}h(y)\right| \leqslant C\vartheta^{s+(x,y)}, \quad x, y \in W_1'$$

where $\mathcal{J}h$ is the Jacobian of h;

4. *SRB measure.* $\tilde{\mu}$ is an SRB measure, i.e. the induced measure $\tilde{\mu}_{W^u}$ on any unstable manifold W^u is absolutely continuous with respect to Leb_{W^u}. We also assume that $\tilde{\mu}$ and is mixing.

5. *One-step expansion.* Let ξ^n denote the partition of M into connected components of $M \backslash \mathcal{S}_n^+$. Denote as V_α the connected component of TW with index

$\alpha \in M/\xi^1$ and $W_\alpha = T^{-1}V_\alpha$. $\exists\ q \in (0,1]$ such that

$$\liminf_{\delta\to 0} \sup_{W:|W|<\delta} \sum_{\alpha\in M/\xi^1} \left(\frac{|W|}{|V_\alpha|}\right)^q \frac{|W_\alpha|}{|W|} < 1,$$

where the supremum is taken over all unstable curves W.

Theorem 13 ([5, 6]). *Under the assumptions 1-5 above, the system (T, M) above enjoys exponential decay of correlations and central limit theorem for dynamically Hölder continuous observables.*

The verifications of Assumptions 1-5 are rather long. Moreover, their validity is of independent importance themselves. So we first state intermediary lemmata in Section 4.4.2, then we prove, based on these lemmata, Theorems 5, 6 and 10 in Section 4.4.3. Finally we prove all the lemmata in Section 4.4.4.

4.4.2 Intermediary Lemmas

In this section we list the intermediate lemmata. Their proofs are presented in Section 4.4.4.

Suppose W is an unstable curve, i.e. the tangent line of W lies in the unstable cone $\mathcal{C}^u$, with bounded curvature. We assume without loss of generality that $W \cap \mathcal{S}^+ = \varnothing$. Let $\mathcal{J}_W(x) = |D_x T|_W|$ denote the Jacobian of $\tilde{F}_\infty$ at $x \in W$. We have the following enhanced distortion control:

Lemma 4.4.1 (Distortion Control). *Suppose W is an unstable curve with bounded curvature. Then for any $x, y \in W$, there exists a constant C which depends only on*

$\tilde{F}_\infty$ such that

$$\left|\log \mathcal{J}_W(x) - \log \mathcal{J}_W(y)\right| \leqslant Cd(x,y).$$

Furthermore, if $W \cap \mathcal{S}_N^- = \varnothing$, then for any $1 \leqslant n \leqslant N$ there exists a constant C' which depends only on $\tilde{F}_\infty$ such that

$$\left|\log \mathcal{J}_W \tilde{F}_\infty^{-n}(x) - \log \mathcal{J}_W \tilde{F}_\infty^{-n}(y)\right| \leqslant C'|W|.$$

In order to establish the N_0-step expansion, we need the following estimate on the speed of fragmentation of unstable curves:

Lemma 4.4.2 (Complexity Bound)**.** *Suppose z is a multiple point of $\mathcal{S}_n^+$. Pick a small neighborhood of z and denote as $k_n(z)$ the number of sectors in the small neighborhood cut out by $\mathcal{S}_n^+$. Then $k_n(z) \leqslant 6n$.*

The linear complexity bound guarantees that a sufficiently short unstable curve W can break into at most $6n$ connected components under $\tilde{F}_\infty^n$. Thus there exists δ_0 so small that any unstable curve shorter than δ_0 satisfies the following expansion estimate:

Lemma 4.4.3 (N_0-Step Expansion)**.** *Suppose that W is an unstable curve with length $|W| \leqslant \delta_0$ and that $\{W_i^n\}_i$ are the connected components of the image $\tilde{F}_\infty^n W$. Denote as $\Lambda_{i,n}$ the minimum rate of expansion on each preimage $\tilde{F}_\infty^{-n} W_i^n$. Then*

$$\sum_i \frac{1}{\Lambda_{i,N_0}} < 1,$$

where N_0 *is the smallest integer such that* $\dfrac{6N_0}{\Lambda^{N_0}} < 1$ *and* Λ *is the expansion rate of* $\tilde{F}_\infty$.

Next, we suppose that W and $\bar{W}$ are two unstable curves with bounded curvatures. We define the following holonomy map h on

$$W' = \{x \in W : W^s(x) \cap \bar{W} \neq \varnothing\}$$

by sliding along the stable manifold from $x \in W$ to $\bar{x} \in \bar{W}$. Then $h : W' \to \bar{W}'$ is absolutely continuous with well-behaving density:

Lemma 4.4.4 (Absolute Continuity)**.** *Suppose* W *and* $\bar{W}$ *are two unstable curves with bounded curvatures. Then* $h_\star \mu_W \ll \mu_{\bar{W}}$ *and that for some constant* C *and* $\Theta < 1$

$$\left|\log \mathcal{J}h(x) - \log \mathcal{J}h(y)\right| \leqslant C\Theta^{s_+(x,y)}, \quad x, y \in W'$$

where $\mathcal{J}h$ *is the Jacobian of* h.

Finally we provide an estimate on the number of small unstable curves, which follows from Lemma 7 in [6].

Suppose W is an unstable curve with length $|W| < \delta_0$. For any $x \in W$, we denote as $r_n(x)$ the distance from x to the nearest boundary of the connected component of $\tilde{F}_\infty^n W$ containing $\tilde{F}_\infty^n x$.

Lemma 4.4.5 (Growth Lemma)**.** *Suppose* W *is an unstable curve with length* $|W| <$

δ_0. *Then for any* $\epsilon > 0$,

$$mes_W\{r_{nN_0}(x) < \epsilon\} \leqslant (\vartheta_1 \Lambda^{N_0})^n mes_W \left\{ r_0(x) < \frac{\epsilon}{\Lambda^{nN_0}} \right\} + C\epsilon|W|$$

where $\vartheta_1 = e^{C'\delta_0} \sum_i \frac{1}{\Lambda_{i,N_0}}$, C' *is the constant from Lemma 4.4.1,* N_0 *is the constant from Lemma 4.4.3 and* Λ *is the expansion rate of* $\tilde{F}_\infty$.

Remark 4.4.6. We note that ϑ_1 can be made less than 1 by choosing δ_0 sufficiently small.

4.4.3 Exponential Decay of Correlations, CLT and Global Global Mixing

In this section we present the proof of Theorem 5, 6 and 10, based on the lemmas from Section 4.4.2.

We start with the proof for exponentially decay of correlations and CLT.

Proof of Theorem 5 and Theorem 6. Firstly we establish the exponential decay and CLT for $\tilde{F}_\infty^{N_0}$ by checking the conditions in Theorem 13 for $\tilde{F}_\infty^{N_0}$ where N_0 is the number from Lemma 4.4.3. Note that we gain from Theorem 13 the exponential decay and CLT for $\tilde{F}_\infty^{N_0}$ rather than for $\tilde{F}_\infty$ because we can only obtain N_0-step expansion on $\tilde{F}_\infty$. Nevertheless, it suffices to prove CLT for $\tilde{F}_\infty^{N_0}$ since the CLT for $\tilde{F}_\infty$ follows easily from that of $\tilde{F}_\infty^{N_0}$.

The proof for the case $\ddot{f} > 0$ is very similar to that for $\ddot{f} < -g$, and thence we omit the latter. Although the positive/negative cones in the proof of Theorem

3 are strictly invariant, we cannot use them here since we require a positive angle between the unstable and stable cones. Instead, we consider their images, i.e.

$$\mathcal{C}^u(\tilde{t}_0, \tilde{v}_0) = \left\{ 2k_0 \leqslant \frac{\delta v}{\delta t} \leqslant 2k_0 + \frac{g}{2} \right\}$$

$$\mathcal{C}^s(\tilde{t}_0, \tilde{v}_0) = \left\{ -\frac{g}{2} \leqslant \frac{\delta v}{\delta t} \leqslant -\frac{2k_0}{\frac{4k_0}{g} + 1} \right\}.$$

It is easy to see that the angles between $\mathcal{C}^u$ and $\mathcal{C}^s$ are uniformly bounded away from zero since $k_0 > 0$ is bounded, and that these cones are strictly invariant.

We now compute the expansion rate Λ. With the same notations as above, for $(\delta t, \delta v) \in \mathcal{C}^u(\tilde{t}_0, \tilde{v}_0)$ it follows from (4.2) that

$$\bar{\delta t}^2 + \bar{\delta v}^2 \geqslant \Lambda_1^2(\delta t^2 + \delta v^2)$$

where $\Lambda_1^2 = \min\left\{ 1 + 4k_{min}, \frac{4}{g^2} + \left(1 + \frac{4k_{min}}{g}\right)^2 \right\} > 1.$

Similarly for $(\delta t, \delta v) \in \mathcal{C}^s(\tilde{t}_0, \tilde{v}_0)$

$$\begin{aligned} \tilde{\delta t}^2 + \tilde{\delta v}^2 &= \left(4k_1^2 + \left(1 + \frac{4k_1}{g}\right)^2\right)\delta t^2 + \left(\frac{4}{g^2} + 1\right)\delta v^2 - 2\left(2k_1 + \frac{2}{g}\left(1 + \frac{4k_1}{g}\right)\right)\delta t \delta v \\ &\geqslant \Lambda_2^2(\delta t^2 + \delta v^2) \end{aligned}$$

where $\Lambda_2^2 = \min\left\{ 4k_{min}^2 + \left(1 + \frac{4k_{min}}{g}\right)^2, \frac{4}{g^2} + 1 \right\} > 1.$

Take $\Lambda = \min\{\Lambda_1, \Lambda_2\}$, and this gives our expansion rate.

Next we examine the singularity curves $\mathcal{S}^{\pm}$.

Observe that $\tilde{F}_\infty$ is a C^2-diffeomorphism away from singularities if f is piece-

wise C^3. And $\mathcal{S}_0 \cup \mathcal{S}^+$ is a finite union of smooth compact curves on the torus $\mathbb{T}$. $\mathcal{S}_0$ is transverse to $\mathcal{C}^u/\mathcal{C}^s$. Moreover the singularity curves are regular and properly aligned as shown in the proof of Theorem 3.

Assumption 2(d) is trivially satisfied since the norm of the derivative $d\tilde{F}_\infty$ is bounded and our phase space is compact.

As for Assumption 3, we have already obtained distortion control in Lemma 4.4.1 and absolute continuity of holonomy map in Lemma 4.4.4. We note that by (4.6) the curvature of an unstable curve remains bounded after iterations.

Next, the invariant measure $\tilde{\mu} = d\tilde{t}d\tilde{v}$ is apparently an SRB measure.

Note that $\tilde{F}_\infty^n$ is ergodic with respect to $\tilde{\mu}$ for any $n > 0$, since $\tilde{F}_\infty^n$ also satisfies the conditions of Theorem 12. Now the results of [35] imply that $\tilde{\mu}$ is mixing (even Bernoulli).

Finally, since we already establish N_0-step expansion from Lemma 4.4.3, we conclude from Theorem 13 that $\tilde{F}_\infty^{N_0}$ enjoys exponential decay of correlations and CLT for dynamically Hölder continuous observables.

The CLT for $\tilde{F}_\infty$ follows easily from that of $\tilde{F}_\infty^{N_0}$. Now we show that exponential mixing for $\tilde{F}_\infty^{N_0}$ implies exponential mixing for $\tilde{F}_\infty$.

Suppose φ, ϕ are two dynamically Hölder continuous observables. For any integer $n \in \mathbb{N}$, $n = pN_0 + q$ for some integers $p > 0$ and $0 \leqslant q < N_0$.

We denote as $\tilde{\varphi}_q = \varphi \circ \tilde{F}_\infty^q$. For any x, y on a same unstable manifold W^u,

$$\left|\tilde{\varphi}_q(x) - \tilde{\varphi}_q(y)\right| = \left|\varphi(\tilde{F}_\infty^q x) - \varphi(\tilde{F}_\infty^q y)\right| \leqslant C\vartheta^{-q_+}\vartheta^{s_+(x,y)}$$

where $q_+ = \min\{q, s_+(x,y)\}$.

On the other hand, for any x, y on a same stable manifold W^s,

$$\left|\tilde{\varphi}_q(x) - \tilde{\varphi}_q(y)\right| = \left|\varphi(\tilde{F}_\infty^q x) - \varphi(\tilde{F}_\infty^q y)\right| \leqslant C\vartheta^q \vartheta^{s_-(x,y)}.$$

Therefore $\tilde{\varphi}_q$ is also dynamically Hölder.

By applying the previous exponential decay result on $\tilde{F}_\infty^{N_0}$ with the observables $\tilde{\varphi}_q, \phi$, we know that $\exists\ C_{\tilde{\varphi}_q,\phi}$ and b such that

$$\begin{aligned}\left|\int_{\mathbb{T}} \left(\varphi \circ \tilde{F}_\infty^n\right)\phi d\tilde{\mu} - \int_{\mathbb{T}} \varphi d\tilde{\mu} \int_{\mathbb{T}} \phi d\tilde{\mu}\right| &= \left|\int_{\mathbb{T}} \left(\tilde{\varphi}_q \circ \tilde{F}_\infty^{pN_0}\right)\phi d\tilde{\mu} - \int_{\mathbb{T}} \tilde{\varphi}_q d\tilde{\mu} \int_{\mathbb{T}} \phi d\tilde{\mu}\right| \\ &\leqslant C_{\tilde{\varphi}_q,\phi} e^{-bp} = C_{\tilde{\varphi}_q,\phi} e^{bq/N_0} (e^{-b/N_0})^n.\end{aligned}$$

If we take $C_{\varphi,\phi} = \max_q \{C_{\tilde{\varphi}_q,\phi} e^{bq/N_0}\}$ and replace b with b/N_0, then we have proved exponential decay of correlation in the case $\ddot{f} > 0$. □

Next we prove the global global mixing property for the original collision map F.

Proof of Theorem 10. Under Assumptions 1-5, the limit map $\tilde{F}_\infty$ satisfies the conditions of [4], thus it admits a Young tower with exponential tail. We recall from Section 4.1.2 that $\tilde{F}_\infty$ well approximates the original collision map F at infinity. Therefore by Theorem 2.4 and 2.9 in [15], F is global global mixing. □

4.4.4 Proof of Intermediary Lemmas

In this section we prove the lemmas stated in Section 4.4.2.

We start with the distortion control.

Proof of Lemma 4.4.1. We parametrize the unstable W as $v = \psi(t)$ for some smooth function ψ such that $\psi'(t) \in [2k, 2k + g/2]$ and ψ'' is bounded.

For $x, y \in W$, $|\log \mathcal{J}_W(x) - \log \mathcal{J}_W(y)| \leqslant \max_{z \in W} \left| \frac{d}{dz} \log \mathcal{J}_W(z) \right| |x - y|$.

For $z \in W$, we take $\mathrm{v} = (1, \psi'(\mathrm{t})) \in \mathcal{T}_{\mathrm{z}}\mathrm{W}$.

$$\mathcal{J}_W(z) = \frac{\left\| d_z \tilde{F}_\infty \mathrm{v} \right\|}{\|\mathrm{v}\|} =$$

$$\frac{1}{\sqrt{1+\psi'(t)^2}} \left(1 + 4k_1^2 + \psi'(t)^2 \left(\frac{4}{g^2} + \left(1 + \frac{4k_1}{g} \right)^2 \right) + 2\psi'(t) \left(\frac{2}{g} + 2k_1 \left(1 + \frac{4k_1}{g} \right) \right) \right)^{1/2}$$

where $k_1 = \ddot{f}(\tilde{F}_\infty z)$. Hence

$$\log \mathcal{J}_W(z) =$$

$$\frac{1}{2} \log \left(1 + 4k_1^2 + \psi'(t)^2 \left(\frac{4}{g^2} + \left(1 + \frac{4k_1}{g} \right)^2 \right) + 2\psi'(t) \left(\frac{2}{g} + 2k_1 \left(1 + \frac{4k_1}{g} \right) \right) \right)$$

$$- \frac{1}{2} \log(1 + \psi'(t)^2). \tag{4.5}$$

We note that each term inside the logarithms in (4.5) is greater than one and has bounded derivatives. Thus $\left| \frac{d}{dz} \log \mathcal{J}_W(z) \right| \leqslant C$ for some constant C depending only on $\tilde{F}_\infty$.

Besides the above distortion bound, we have the following enhanced estimate.

Now we assume further that $W \cap \mathcal{S}_n^- = \varnothing$.

We denote $x_n = \tilde{F}_\infty^{-n} x$, $y_n = \tilde{F}_\infty^{-n} y$ and $W_n = \tilde{F}_\infty^{-n} W$.

$$\begin{aligned}\left|\log \mathcal{J}_W \tilde{F}_\infty^{-n}(x) - \log \mathcal{J}_W \tilde{F}_\infty^{-n}(y)\right| &\leqslant \sum_{m=0}^{n-1} \left|\log \mathcal{J}_{W_m} \tilde{F}_\infty^{-n}(x_m) - \log \mathcal{J}_{W_m} \tilde{F}_\infty^{-n}(y_m)\right| \\ &\leqslant \sum_{m=0}^{n-1} |W_m| \max_{z_m \in W_m} \left|\frac{d}{dz_m} \log \mathcal{J}_{W_m} \tilde{F}_\infty^{-1}(z_m)\right|.\end{aligned}$$

But

$$\begin{aligned}\frac{d}{dz_m} \log \mathcal{J}_{W_m} \tilde{F}_\infty^{-1}(z_m) &= \frac{dz_{m+1}}{dz_m} \frac{d}{dz_{m+1}} \log \frac{1}{\mathcal{J}_{W_{m+1}} \tilde{F}_\infty(z_{m+1})} \\ &= -\frac{1}{\mathcal{J}_{W_{m+1}} \tilde{F}_\infty(z_{m+1})} \frac{d}{dz_{m+1}} \log \mathcal{J}_{W_{m+1}} \tilde{F}_\infty(z_{m+1}).\end{aligned}$$

Observe that $\mathcal{J}_{W_{m+1}} \tilde{F}_\infty(z_{m+1})$ is bounded. Next

$$\frac{dv_m}{dt_m} = \frac{2k_m dt_{m-1} + (4k_m/g + 1) dv_{m-1}}{dt_{m-1} + \frac{2}{g} dv_{m-1}}$$

$$= \frac{2k_m + (4k_m/g + 1)\frac{dv_{m-1}}{dt_{m-1}}}{1 + \frac{2}{g}\frac{dv_{m-1}}{dt_{m-1}}} = 2k_m + g/2 - \frac{g/2}{1 + \frac{2}{g}\frac{dv_{m-1}}{dt_{m-1}}}.$$

Therefore

$$\psi''_m = 2\dddot{f}(t_m) - \frac{\psi''_{m-1}}{\left(1 + \frac{2}{g}\psi'_{m-1}\right)^3}$$

which implies that

$$|\psi''_m| \leqslant 2\dddot{f}_{\max} + \theta |\psi''_{m-1}|$$

where $\theta := \frac{1}{(1+4k_{\min}/g)^3} < 1$. Iterating we obtain

$$|\psi''_m| \leqslant \frac{2\dddot{f}_{\max}}{1-\theta} + \theta^m |\psi''_0|. \tag{4.6}$$

Hence $\left|\frac{d}{dz_{m+1}} \log \mathcal{J}_{W_{m+1}} \tilde{F}_\infty(z_{m+1})\right|$ is bounded. Thus

$$\left|\log \mathcal{J}_W \tilde{F}_\infty^{-n}(x) - \log \mathcal{J}_W \tilde{F}_\infty^{-n}(y)\right| \leqslant C'' \sum_{m=0}^{n-1} |W_m| \leqslant C'' \sum_{m=0}^{n-1} \frac{|W|}{\Lambda^m} \leqslant C'|W|. \qquad \square$$

Next we prove the complexity bound following an approach of [9].

Proof of Lemma 4.4.2. Suppose z is a multiple point of $\mathcal{S}_n^+$. We take a small neighborhood of z and cut it into four quadrants Q's by vertical and horizontal lines through z. Denote as $k_n(z)|_Q$ the number of sectors cut out by $\mathcal{S}_n^+$ intersecting nontrivially with Q.

We are only interested in the active quadrants, i.e. the quadrants in the northwest and southeast, because the tangent lines to the singularities curves $\mathcal{S}_n^+$ have negative slopes and the inactive quadrants (in the northeast and southwest) remain untouched by them and thus do not contribute to the complexity growth.

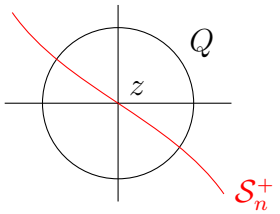

Figure 4.1: A multiple point and its sectors

Denote as $\{V_i\}$ the sectors cut out by $\mathcal{S}^+$. Note that $\mathcal{S}^+ = \{\tilde{t}_1 = 0\}$, hence there are at most two sectors cut out by $\mathcal{S}^+$ in a quadrant. By further cutting

horizontally and vertically, we might assume each $V_i \subseteq Q$.

We denote as $V_i' = \tilde{F}_\infty(V_i)$, $z_i' = \tilde{F}_\infty(z_i)$ (this is defined by continuity), and $k_n(z)|_Q = \sum_i k_{n-1}(z_i')|V_i'$.

If $z \notin \mathcal{S}^+$, then $i = 1$ and $k_n(z)|_Q = k_{n-1}(z')|V'$. If $z \in \mathcal{S}^+$, then $i = 2$ and we claim that at most one image V_i' of the sectors V_i remains active, so that in both cases we have

$$\begin{aligned} k_n(z)|_Q &= \sum_i k_{n-1}(z_i')|V_i' \\ &\leqslant 1 + k_{n-1}(z_i')|V_i' \text{ (V_i' is the only active image)} \\ &\leqslant 3 + k_{n-1}(z_i')|Q_i' \text{ (by further cutting V_i' horizontally and vertically).} \end{aligned}$$

Thus $k_n(z)|_Q \leqslant 3n$ implies $k_n(z) \leqslant 6n$, which is our desired complexity bound.

Now we prove our claim. Suppose that $z \in \{\tilde{t}_1 = 0\}$.

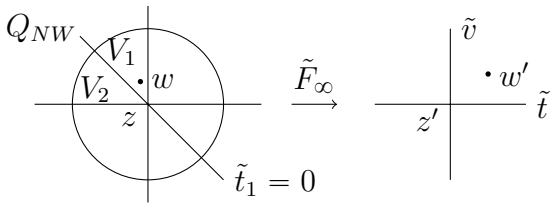

Figure 4.2: Northwest quadrant for $z \in \{\tilde{t}_1 = 0\}$

Recall that $\tilde{t}_1 = \tilde{t}_0 + \frac{2\tilde{v}_0}{g} \pmod 1$, $\tilde{v}_1 = \tilde{v}_0 + 2\dot{f}(\tilde{t}_1) \pmod g$.

Since $z \in \{\tilde{t}_1 = 0\}$, the $\tilde{t}$-coordinate of its images z' is zero, i,e. $\tilde{t}(z_i') = 0$ $(i = 1, 2)$.

We pick $w \in V_1$ sufficiently close to z, then the $\tilde{t}$-coordinate of its image w' is positive since w is at the right side of the singularity line $\{\tilde{t}_1 = 0\}$. Also, since we

assume $\ddot{f} > 0$, $\dot{f}$ is increasing and hence the $\tilde{v}$-coordinate of its image w' is larger than that of z'. This means that the image $V_1' = \tilde{F}_\infty(V_1)$ is inactive.

Similarly, we can show that the lower one to the left of the singularity line $\mathcal{S}^+$ in the southeast quadrant becomes inactive after being mapped by $\tilde{F}_\infty$. □

Finally we estimate the Jacobian of the holonomy map.

Proof of Lemma 4.4.4. It follows from classical results in [1, 41] that the holonomy map is absolutely continuous and its Jacobian is given by

$$\mathcal{J}h(x) = \prod_{j=0}^{\infty} \frac{\mathcal{J}_{W_j}(x_j)}{\mathcal{J}_{\bar{W}_j}(\bar{x}_j)}$$

where $W_j/\bar{W}_j = \tilde{F}_\infty^j W/\tilde{F}_\infty^j \bar{W}$ and $x_j/\bar{x}_j = \tilde{F}_\infty^j x/\tilde{F}_\infty^j \bar{x}$.

As a result,

$$\log \mathcal{J}h(x) = \sum_{j=0}^{\infty} \log \mathcal{J}_{W_j}(x_j) - \log \mathcal{J}_{\bar{W}_j}(\bar{x}_j).$$

Since $\psi' \in [2k, 2k + \frac{g}{2}]$, we obtain by (4.5)

$$
\begin{aligned}
&2|\log \mathcal{J}_{W_j}(x_j) - \log \mathcal{J}_{\bar{W}_j}(\bar{x}_j)| \\
\leqslant &\left| \log \left(1 + 4k_{j+1}^2 + \psi_j'^2 \left(\frac{4}{g^2} + \left(1 + \frac{4k_{j+1}}{g} \right)^2 \right) + 2\psi_j' \left(\frac{2}{g} + 2k_{j+1} \left(1 + \frac{4k_{j+1}}{g} \right) \right) \right) \right. \\
&\left. - \log \left(1 + 4\bar{k}_{j+1}^2 + \bar{\psi}_j'^2 \left(\frac{4}{g^2} + \left(1 + \frac{4\bar{k}_{j+1}}{g} \right)^2 \right) + 2\bar{\psi}_j' \left(\frac{2}{g} + 2\bar{k}_{j+1} \left(1 + \frac{4\bar{k}_{j+1}}{g} \right) \right) \right) \right| \\
&+ |\log(1 + \psi_j'^2) + \log(1 + \bar{\psi}_j'^2)| \\
\leqslant &C\theta_1(|k_{j+1} - \bar{k}_{j+1}| + |\psi_j' - \bar{\psi}_j'|) + C\theta_2|\psi_j' - \bar{\psi}_j'| \\
\leqslant &C\theta_1(|t_{j+1} - \bar{t}_{j+1}| + |\psi_j' - \bar{\psi}_j'|) + C\theta_2|\psi_j' - \bar{\psi}_j'|
\end{aligned}
$$

where

$$
\theta_1^{-1/2} = 1 + 4k_{\min}^2 + 4k_{\min}^2 \left(\frac{4}{g^2} + \left(1 + \frac{4k_{\min}}{g} \right)^2 \right) + 4k_{\min} \left(\frac{2}{g} + 2k_{\min} \left(1 + \frac{4k_{\min}}{g} \right) \right) > 1,
$$

$$
\theta_2^{-1/2} = 1 + 4k_{\min}^2 > 1.
$$

It also follows from (4.3) that

$$\begin{aligned}
|\psi'_j - \bar{\psi}'_j| &\leqslant C|t_j - \bar{t}_j| + C\theta_3|\psi'_{j-1} - \bar{\psi}'_{j-1}| \\
&\leqslant C|t_j - \bar{t}_j| + C\theta_3|t_{j-1} - \bar{t}_{j-1}| + C\theta_3^2|\psi'_{j-2} - \bar{\psi}'_{j-2}| \\
&\cdots \\
&\leqslant C|t_j - \bar{t}_j| + C\theta_3|t_{j-1} - \bar{t}_{j-1}| + \cdots + C\theta_3^{j-1}|t_1 - \bar{t}_1| + C\theta_3^j|\psi'_0 - \bar{\psi}'_0| \\
&\leqslant C\frac{|t_0 - \bar{t}_0|}{\Lambda^n} + C\theta_3\frac{|t_0 - \bar{t}_0|}{\Lambda^{j-1}} + \cdots + C\theta_3^{j-1}\frac{|t_0 - \bar{t}_0|}{\Lambda} + C\theta_3^j|\psi'_0 - \bar{\psi}'_0| \\
&\leqslant Cj\theta_4^j|t_0 - \bar{t}_0| + C\theta_3^j|\psi'_0 - \bar{\psi}'_0|
\end{aligned}$$

where $\theta_3^{-1/2} = 1 + 4k_{\min}/g > 1$, $\theta_4 = \max\{\theta_3, \Lambda^{-1}\} < 1$ and Λ is the expansion rate of unstable curves.

Consequently,

$$|\log \mathcal{J}_{W_j}(x_j) - \log \mathcal{J}_{\bar{W}_j}(\bar{x}_j)| \leqslant Cj\Theta^j|t_0 - \bar{t}_0| + C\Theta^j|\psi'_0 - \bar{\psi}'_0| \tag{4.7}$$

where $\Theta = \max\{\theta_1, \theta_2, \theta_3, \theta_4\} < 1$.

Finally we are ready to estimate the Jacobian. Observe that $s_+(x, y) = s_+(\bar{x}, \bar{y})$ since each pair $(x, \bar{x})$, $(y, \bar{y})$ is connected by its corresponding stable manifold.

$$\begin{aligned}
&|\log \mathcal{J}h(x) - \log \mathcal{J}(y)| \\
&\leqslant \sum_{j=0}^{\infty} |\log \mathcal{J}_{W_j}(x_j) - \log \mathcal{J}_{\bar{W}_j}(\bar{x}_j) - \log \mathcal{J}_{W_j}(y_j) + \log \mathcal{J}_{\bar{W}_j}(\bar{y}_j)|
\end{aligned}$$

$$\leqslant \sum_{j<s_+(x,y)} \left(|\log \mathcal{J}_{W_j}(x_j) - \log \mathcal{J}_{W_j}(y_j)| + |\log \mathcal{J}_{\bar{W}_j}(\bar{x}_j) - \log \mathcal{J}_{\bar{W}_j}(\bar{y}_j)|\right)$$

$$+ \sum_{j\geqslant s_+(x,y)} \left(|\log \mathcal{J}_{W_j}(x_j) - \log \mathcal{J}_{\bar{W}_j}(\bar{x}_j)| + |\log \mathcal{J}_{W_j}(y_j) - \log \mathcal{J}_{\bar{W}_j}(\bar{y}_j)|\right)$$

$$\leqslant C \sum_{j<s_+(x,y)} (|x_j - \bar{x}_j| + |y_j - \bar{y}_j|) + C \sum_{j\geqslant s_+(x,y)} j\Theta^j(|x_0 - \bar{x}_0| + |y_0 - \bar{y}_0|)$$

$$+\Theta^j(|\psi'(x_0) - \bar{\psi}'(\bar{x}_0)| + |\psi'(y_0) - \bar{\psi}'(\bar{y}_0)|)$$

$$\leqslant C\Lambda^{-s_+(x,y)}(|x_{s_+(x,y)} - \bar{x}_{s_+(x,y)}| + |y_{s_+(x,y)} - \bar{y}_{s_+(x,y)}|)$$

$$+\Theta^{s_+(x,y)}(|x_0 - \bar{x}_0| + |y_0 - \bar{y}_0| + |\psi'(x_0) - \bar{\psi}'(\bar{x}_0)| + |\psi'(y_0) - \bar{\psi}'(\bar{y}_0)|) \leqslant C\Theta^{s_+(x,y)}$$

where the sum of small indices $j < s_+(x,y)$ is controlled by the distortion estimate from Lemma 4.4.1 and the sum of large indices $j \geqslant s_+(x,y)$ is controlled by (4.7). □

4.5 Escaping and Bounded Orbits

Theorem 7 shows that the escaping orbits takes up a null set. However in this section we show that the escaping orbits do exist and so do the bounded orbits.

We introduce the notion of *proper standard pair*. A *standard pair* (W, μ_W) consists of an unstable curve W and a *regular* probability measure μ_W supported on W, i.e. μ_W is absolutely continuous and has a dynamically Hölder density. We say a standard pair is *proper* if there exists a large constant C_p bounding the following the quantity

$$\mathcal{Z}_W := \sup_{\epsilon} \frac{\mu_W\{r_0 < \epsilon\}}{\epsilon}.$$

It is easy to see that in our case μ_W is the normalised Lebesgue measure on the

unstable curve and that $\mathcal{Z}_W = \frac{2}{|W|}$, so any unstable curve W longer than δ_2 endowed with Lebesgue measure is a proper standard pair. We also observe that δ_2 can be made arbitrarily small by choosing C_p large. Therefore by Theorem 5 and Lemma 2.2, 2.3 in [14], we have the following central limit theorem for all proper standard pairs:

Proposition 4.5.1. *There exists $\delta_2 \gg 1$ such that on any unstable curve W with $|W| > \delta_2$ we have the following central limit theorem for dynamically Hölder observables, i.e.*

$$\frac{1}{\sqrt{n}} \sum_{i=0}^{n-1} \varphi \circ \tilde{F}_\infty^i \overset{dist}{\rightarrow} \mathcal{N}(0, \sigma_\varphi^2)$$

where φ is dynamically Hölder with zero average $\int_{\mathbb{T}} \varphi d\tilde{\mu} = 0$.

Now we prove Theorem 9.

Proof of Theorem 9. Let us denote $(t_n^\infty, v_n^\infty) = F_\infty^n(t_0, v_0)$ and $(t_n, v_n) = F^n(t_0, v_0)$.

First we recall from Section 4.3 that the energy change γ in the limit map F_∞ on the cylinder has zero average. Moreover, γ is dynamically Hölder as it is piecewise C^1 and its discontinuities are located exactly on $\mathcal{S}^+$. Therefore by Proposition 4.5.1, $\exists n_0, A$ such that for every unstable curve W longer than δ_2

$$\mathbb{P}_W \left(v_{n_0 N_0}^\infty > v_0 + A\sqrt{n_0 N_0} \right) > \frac{1}{3}$$

where N_0 is the constant from Lemma 4.4.3 N_0-Step Expansion.

By Lemma 4.4.5, if δ_2 is sufficiently small, then for sufficiently large n_0

$$\mathbb{P}_W(r_{n_0N_0} < 4\delta_2) < \frac{1}{10}.$$

We know from Section 4.1.2 that the limit map F_∞ well approximates the original collision map F for large velocity with an error of order $\mathcal{O}(v_0^{-1})$ on each continuity component of $F_\infty^{n_0N_0}W$, thus we can choose $v_* \gg 1$ so large that if $v_0 > v_*$ everywhere on W, then we have

$$\mathcal{P}_W(v_{n_0N_0} > v_0 + A\sqrt{n_0N_0}, r_{n_0N_0} > 4\delta_2) > \frac{1}{4}.$$

By the estimate above, at least one component $W_1 \subset F_\infty^{n_0N_0}W$ contains a segment $\bar{W}_1$ longer than δ_2 and $v_{n_0N_0} > v_0 + A\sqrt{n_0N_0}$ holds everywhere on $\bar{W}_1$. By repeating the argument on $\bar{W}_1$, we get another component $W_2 \subset F_\infty^{n_0N_0}\bar{W}_1$ containing a segment $\bar{W}_2$ longer than δ_2 and the velocity increases by another $A\sqrt{n_0N_0}$. Inductively, we construct an escaping orbit.

Similarly, we can construct an orbit whose velocity first increases by $A\sqrt{n_0N_0}$ and then decreases by $A\sqrt{n_0N_0}$ and etc. In that way we obtain an orbit whose energy remains in $[v_0 - 2A\sqrt{n_0N_0}, v_0 + 2A\sqrt{n_0N_0}]$. This holds for arbitrarily large $v_0 > v_*$, thus we have bounded orbits at arbitrarily high energy level. □

Bibliography

[1] D. V. Anosov and Y. G. Sinai. Some smooth ergodic systems. *Russian Mathematical Surveys*, 22(5):103–167, 1967.

[2] M. Arnold and V. Zharnitsky. Pinball dynamics: unlimited energy growth in switching Hamiltonian systems. *Comm. Math. Phys.*, 338(2):501–521, 2015.

[3] J. R. Cary, D. F. Escande, and J. L. Tennyson. Change of the adiabatic invariant due to separatrix crossing. *Phys. Rev. Lett.*, 56(20):2117–2120, 1986.

[4] J. Chen, F. Wang, and H.-K. Zhang. Markov partition and thermodynamic formalism for hyperbolic systems with singularities, 2019. `arXiv:1709.00527`.

[5] N. Chernov. Decay of correlations and dispersing billiards. *J. Statist. Phys.*, 94(3-4):513–556, 1999.

[6] N. Chernov and H.-K. Zhang. On statistical properties of hyperbolic systems with singularities. *Journal of Statistical Physics*, 136(4):615–642, 2009.

[7] J. de Simoi. Stability and instability results in a model of Fermi acceleration. *Discrete Contin. Dyn. Syst.*, 25(3):719–750, 2009.

[8] J. de Simoi and D. Dolgopyat. Dynamics of some piecewise smooth Fermi–Ulam models. *Chaos: An Interdisciplinary Journal of Nonlinear Science*, 22(2):026124, 2012.

[9] J. de Simoi and I. P. Toth. An expansion estimate for dispersing planar billiards with corner points. *Ann. Henri Poincaré*, 15(6):1223–1243, 2014.

[10] D. Dolgopyat. Lectures on bouncing balls. `http://www-users.math.umd.edu/~dolgop/BBNotes.pdf`.

[11] D. Dolgopyat. Bouncing balls in non-linear potentials. *Discrete Contin. Dyn. Syst.*, 22(1-2):165–182, 2008.

[12] D. Dolgopyat. Fermi acceleration. In *Geometric and probabilistic structures in dynamics*, volume 469 of *Contemp. Math.*, pages 149–166. Amer. Math. Soc., Providence, RI, 2008.

[13] D. Dolgopyat. Piecewise smooth perturbations of integrable systems. In *XVIIth International Congress on Mathematical Physics*, pages 52–66. World Sci. Publ., Hackensack, NJ, 2014.

[14] D. Dolgopyat and P. Nándori. Nonequilibrium density profiles in Lorentz tubes with thermostated boundaries. *Comm. Pure Appl. Math.*, 69(4):649–692, 2016.

[15] D. Dolgopyat and P. Nándori. Infinite measure mixing for some mechanical systems, 2018. arXiv:1812.01174.

[16] B. Fayad and R. Krikorian. Herman's last geometric theorem. *Annales scientifiques de l'École Normale Supérieure*, 42(2):193–219, 2009.

[17] E. Fermi. On the origin of the cosmic radiation. *Phys. Rev.*, 75:1169–1174, Apr 1949.

[18] V. Gelfreich, V. Rom-Kedar, K. Shah, and D. Turaev. Robust exponential acceleration in time-dependent billiards. *Physical review letters*, 106:074101, 02 2011.

[19] V. Gelfreich, V. Rom-Kedar, and D. Turaev. Fermi acceleration and adiabatic invariants for non-autonomous billiards. *Chaos*, 22(3):033116, 21, 2012.

[20] V. Gelfreich, V. Rom-Kedar, and D. Turaev. Oscillating mushrooms: adiabatic theory for a non-ergodic system. *J. Phys. A*, 47(39):395101, 21, 2014.

[21] V. Gelfreich and D. Turaev. Fermi acceleration in non-autonomous billiards. *Journal of Physics A: Mathematical and Theoretical*, 41(21):212003, may 2008.

[22] V. Gelfreich and D. Turaev. Unbounded energy growth in hamiltonian systems with a slowly varying parameter. *Commun. Math. Phys.*, 2008.

[23] J. Koiller, R. Markarian, S.O. Kamphorst, and S.P. de Carvalho. Time-dependent billiards. *Nonlinearity*, 8(6):983–1003, nov 1995.

[24] M. Kunze and R. Ortega. Escaping orbits are rare in the quasi-periodic Fermi–Ulam ping-pong. *Ergodic Theory and Dynamical Systems*, 2018.

[25] S. Laederich and M. Levi. Invariant curves and time-dependent potentials. *Ergodic Theory and Dynamical Systems*, 11(2):365–378, 1991.

[26] E.D. Leonel, J. Kamphorst, L. da Silva, and S.O. Kamphorst. On the dynamical properties of a fermi accelerator model. *Physica A: Statistical Mechanics and its Applications*, 331(3):435 – 447, 2004.

[27] M. Levi and J-G You. Oscillatory escape in a duffing equation with a polynomial potential. *J. Differential Equations*, 140(2):415–426, 1997.

[28] M. Levi and E. Zehnder. Boundedness of solutions for quasiperiodic potentials. *SIAM J. Math. Anal.*, 26(5):1233–1256, 1995.

[29] A. J. Lichtenberg, M. A. Lieberman, and R. H. Cohen. Fermi acceleration revisited. *Phys. D*, 1(3):291–305, 1980.

[30] C. Liverani and M. Wojtkowski. Ergodicity in hamilto-nian systems. In *Dynamics Reported: Expositions in Dynamical Systems*, pages 130–202. Berlin, Heidelberg: Springer, 1995.

[31] A. Loskutov, A. B. Ryabov, and L. G. Akinshin. Properties of some chaotic billiards with time-dependent boundaries. *Journal of Physics A: Mathematical and General*, 33(44):7973–7986, oct 2000.

[32] A. I. Neĭshtadt. Probability phenomena due to separatrix crossing. *Chaos*, 1(1):42–48, 1991.

[33] R. Ortega. Boundedness in a piecewise linear oscillator and a variant of the small twist theorem. *Proc. London Math. Soc. (3)*, 79(2):381–413, 1999.

[34] R. Ortega. Dynamics of a forced oscillator having an obstacle. In *Variational and topological methods in the study of nonlinear phenomena (Pisa, 2000)*, volume 49 of *Progr. Nonlinear Differential Equations Appl.*, pages 75–87. Birkhäuser Boston, Boston, MA, 2002.

[35] Y. B. Pesin. Dynamical systems with generalized hyperbolic attractors: hyperbolic, ergodic and topological properties. *Ergodic Theory and Dynamical Systems*, 12(1):123–151, 1992.

[36] G. N. Piftankin and D. V. Treshchëv. Separatrix maps in Hamiltonian systems. *Uspekhi Mat. Nauk*, 62(2(374)):3–108, 2007.

[37] L. D. Pustylnikov. Stable and oscillating motions in nonautonomous dynamical systems. II. *Trudy Moskov. Mat. Obšč.*, 34:3–103, 1977.

[38] L. D. Pustylnikov. On Ulam's problem. *Theoret. and Math. Phys.*, 57:1035–1038, 1983.

[39] L. D. Pustylnikov. Existence of invariant curves for maps close to degenerate maps, and a solution of the Fermi–Ulam problem. *Mat. Sb.*, 185:113–124, 1994.

[40] K. Shah, D. Turaev, and V. Rom-Kedar. Exponential energy growth in a Fermi accelerator. *Phys. Rev. E*, 81:056205, May 2010.

[41] Y. G. Sinai. Dynamical systems with elastic reflections. *Russian Mathematical Surveys*, 25(2):137–189, 1970.

[42] S.M. Ulam. On some statistical properties of dynamical systems. In *Proceedings of the Fourth Berkeley Symposium on Mathematical Statistics and Probability, Volume 3: Contributions to Astronomy, Meteorology, and Physics*, pages 315–320, Berkeley, Calif., 1961. University of California Press.

[43] Q. Wang and L.-S. Young. Strange attractors in periodically-kicked limit cycles and Hopf bifurcations. *Comm. Math. Phys.*, 240(3):509–529, 2003.

[44] G. M. Zaslavsky. The simplest case of a strange attractor. *Phys. Lett. A*, 69(3):145–147, 1978/79.

[45] V. Zharnitsky. Instability in Fermi-Ulam ping-pong problem. *Nonlinearity*, 11(6):1481–1487, nov 1998.

[46] V. Zharnitsky. Invariant curve theorem for quasiperiodic twist mappings and stability of motion in the Fermi-Ulam problem. *Nonlinearity*, 13(4):1123–1136, 2000.

[47] J. Zhou. Piecewise smooth fermi-ulam pingpong with potential, 2019. (submitted) Available at `http://arxiv.org/abs/1912.01154`.

[48] J. Zhou. A rectangular billiard with moving slits. *Nonlinearity*, 33(4):1542–1571, Feb 2020.